

87-0326
COMPUTER SYSTEMS LABORATORY

STANFORD UNIVERSITY · STANFORD, CA 94305-2192

AD-A221 821

PERFORMANCE EVALUATION OF CHANNEL ACCESS
SCHEMES IN MULTIHOP PACKET RADIO NETWORKS
WITH REGULAR STRUCTURE BY SIMULATION

Fouad. A. Tobagi and David. H. Shur

CSL Technical Report No. 85-278
SURAN Temporary Note No. 33

June 1985

This work was supported by the Defense Advanced Research Projects Agency under
Contracts MDA 903-79-C-0201 and MDA 903-84-K-0249.

DO NOT REMOVE

ZUAAAAAA26346575

REPORT DOCUMENTATION PAGE		READ INSTRUCTIONS BEFORE COMPLETING FORM
1. REPORT NUMBER 85-278	2. GOVT ACCESSION NO.	3. RECIPIENT'S CATALOG NUMBER
4. TITLE (and Subtitle) PERFORMANCE EVALUATION OF CHANNEL ACCESS SCHEMES IN MULTI-HOP PACKET RADIO NETWORKS WITH REGULAR STRUCTURE BY SIMULATION		5. TYPE OF REPORT & PERIOD COVERED TECHNICAL REPORT
		6. PERFORMING ORG. REPORT NUMBER 85-278
7. AUTHOR(s) F. A. Tobagi and D. H. Shur		8. CONTRACT OR GRANT NUMBER(s) MDA 903-79-C-0201 MDA 903-84-K-0249
9. PERFORMING ORGANIZATION NAME AND ADDRESS Stanford Electronics Laboratory Stanford University Stanford, California 94305-2192		10. PROGRAM ELEMENT, PROJECT, TASK AREA & WORK UNIT NUMBERS
11. CONTROLLING OFFICE NAME AND ADDRESS Defense Advance Research Projects Agency Information Processing Techniques Office 1400 Wilson Blvd., Arlington, VA 22209		12. REPORT DATE June 1985
		13. NUMBER OF PAGES 70
14. MONITORING AGENCY NAME & ADDRESS (if different from Controlling Office) Resident Representative Office of Naval Research Durand 165 Stanford University, Stanford, CA 94305-2192		15. SECURITY CLASS. (of this report) Unclassified
16. DISTRIBUTION STATEMENT (of this Report) Approved for Public Release; Distribution Unlimited		15a. DECLASSIFICATION DOWNGRADING SCHEDULE
17. DISTRIBUTION STATEMENT (of the abstract entered in Block 20, if different from Report)		
18. SUPPLEMENTARY NOTES		
19. KEY WORDS (Continue on reverse side if necessary and identify by block number)		
20. ABSTRACT (Continue on reverse side if necessary and identify by block number) In this report, the performance of various channel access schemes in multi-hop packet radio networks with a regular structure is studied by means of simulation. The channel access schemes considered are: ALOHA (pure and slotted), Carrier Sense Multiple Access (CSMA), Busy Tone Multiple Access (BTMA), Code Division Multiple Access (CDMA), and a new hypothetical scheme introduced here for comparison purposes referred to as Coded Activity Signalling Multiple Access (CASMA). Network throughput and packet de-		

lay are evaluated, as well as the effects on performance of the nodal transmission scheduling rate, the propagation delay among nodes, and to some extent the input flow control. In this study, we consider networks in which both the topology and the traffic pattern are symmetric. This renders all nodes in the network statistically identical, and thus helps reduce the complexity of the simulation task considerably without jeopardizing the objective. The performance of CSMA in such networks is shown to be rather poor as compared with its performance in fully connected networks, while relatively high performance is achieved by the CASMA scheme, the various BTMA protocols, as well as the CDMA scheme, as compared with CSMA and the ALOHA schemes.

Accession For	
NTIS GRA&I	<input checked="" type="checkbox"/>
DTIC TAB	<input type="checkbox"/>
Unannounced	<input type="checkbox"/>
Justification	
By	
Distribution	
Availability	

DTIC

A-1



PERFORMANCE EVALUATION OF CHANNEL ACCESS SCHEMES IN MULTIHOP PACKET RADIO NETWORKS WITH REGULAR STRUCTURE BY SIMULATION*

Fouad. A. Tobagi and David. H. Shur

**CSL Technical Report No. 85-278
SURAN Temporary Note No. 33**

June 1985

Computer Systems Laboratory
STANFORD UNIVERSITY,
Stanford, CA 94305

Abstract

In this report, the performance of various channel access schemes in multihop packet radio networks with a regular structure is studied by means of simulation. The channel access schemes considered are: ALOHA (pure and slotted), Carrier Sense Multiple Access (CSMA), Busy Tone Multiple Access (BTMA), Code Division Multiple Access (CDMA), and a new hypothetical scheme introduced here for comparison purposes referred to as Coded Activity Signalling Multiple Access (CASMA). Network throughput and packet delay are evaluated, as well as the effects on performance of the nodal transmission scheduling rate, the propagation delay among nodes, and to some extent the input flow control. In this study, we consider networks in which both the topology and the traffic pattern are symmetric. This renders all nodes in the network statistically identical, and thus helps reduce the complexity of the simulation task considerably without jeopardizing the objective. The performance of CSMA in such networks is shown to be rather poor as compared with its performance in fully connected networks, while relatively high performance is achieved by the CASMA scheme, the various BTMA protocols, as well as the CDMA scheme, as compared with CSMA and the ALOHA schemes.

Key Words and Phrases: multihop packet radio, channel access protocols, ALOHA, CSMA, busy tone, code division multiple access, performance, throughput, delay.

*This work was supported by the Defense Advanced Research Projects Agency under Contracts MDA 903-79-C-0201 and MDA 903-84-K-0249, monitored by the Office of Naval Research.

Copyright © 1985 Fouad A. Tobagi and David H. Shur

1. Introduction

A packet radio network is a collection of geographically distributed, possibly mobile, packet radio units (PRU's), communicating with each other over a shared broadcast radio channel. Data originates at some PRU's (referred to as sources), is destined for other PRU's (referred to as destinations), and is transmitted in packetized form. Since a radio transmitter may be unable to reach its destination, either due to power limitation or because the topology includes obstacles that are opaque to radio signals, PRU's also act as repeaters which relay packets in a store-and-forward manner between sources and destinations. Thus a message transmitted by the source might travel over many hops before reaching the destination.

There are many variables that need to be considered in the design of packet radio systems. Some of these are determined by the general objectives of the system. For example, all devices employ omnidirectional antennas in order to facilitate communications among mobile users. Other design variables have to be optimally selected so as to achieve the most cost-effective design. Among the variables to be selected are: the network topology, which consists of the number of devices and how they are configured; the modulation and data encoding schemes used on the radio channel; the channel access policy by which the radio devices access the shared radio channel; the routing protocol which determines the paths followed by packets; the flow control protocol which controls the acceptance of packets by nodes of the network; and finally the nodal design which includes the selection of the storage capacity at each node as well as the selection of the buffer management strategy to be used. In this report, we will focus mainly on the study of the performance of various channel access schemes.

Many access schemes have been devised which allow a set of geographically distributed users to access a common channel. As discussed in [1], these schemes differ in several respects; namely, the static or dynamic nature of the bandwidth allocation, the centralized

or distributed nature of the decision making process, and the degree of adaptivity to changes in user demands. Accordingly, they are grouped into different classes among which, given the mobile radio environment, the class of random access techniques offers the desired feature of simplicity in providing access to the channel in a distributed and dynamic fashion. The simplest random access protocol is ALOHA [1,2], which permits users to transmit any time they desire. Under this protocol, the overlap in time and space of several transmissions which may occur on the shared channel may induce significant errors in some or all of these transmissions, thus resulting in low channel efficiency. Carrier sense multiple access (CSMA) attempts to alleviate this problem by requiring the transmitter to sense the state of the channel (busy or idle) prior to transmitting, and to inhibit transmission if the channel is sensed busy [3]. Analyses of these access schemes have previously focused mainly on single hop environments, with the assumption that all nodes are within range and in line-of-sight of each other. In such environments, and when in addition the propagation delay is small compared to the transmission time of a packet, analysis has clearly demonstrated the high channel utilization of CSMA and its superiority over the pure and slotted ALOHA schemes [3]. Analysis, however, has also shown that CSMA suffers severe degradation when *hidden nodes* are present; i.e., when all nodes are not within range and in line-of-sight of each other [4]. This situation is clearly met in multihop packet radio networks, and hence, CSMA is not expected to perform as well in such networks as it does in fully connected networks. The busy tone multiple access scheme (BTMA) attempts to overcome the hidden node problem by having a node transmit a busy tone when it is busy receiving, thus preventing its neighbors from interfering with its reception [4,5]. Clearly, the reduction in interference is obtained at the expense of the increased bandwidth needed for the busy tone.

An alternative solution to the problem of collisions in multiaccess/broadcast networks is based on spread spectrum and code division techniques. When these techniques are utilized, the number of collisions may be reduced by using orthogonal signalling codes

in conjunction with matched filters at the intended receivers. Clearly, here too multiple orthogonal codes are obtained at the expense of increased bandwidth needed in order to spread the waveforms. When both code division signalling techniques and multiaccess protocols for accessing the channel are used, the resulting channel access schemes are known as code division multiple access (CDMA) schemes [6]. One CDMA scheme consists of assigning a unique code to each node; nodes then wishing to transmit to a particular node must utilize the code assigned to that node.

Results obtained to-date on the performance analysis of multihop packet radio networks have been limited in several respects. In particular, the analysis of delay in such networks appears to be an intractable task; and the effect of propagation delay and of the buffering of packets by store-and-forward repeaters have been little studied in the literature. Previous work relevant to the present study is now outlined below. In [7] and [8] the slotted ALOHA and CSMA protocols were analyzed but the topology was restricted to a two hop centralized configuration. In [9] - [14] a Markovian model capable of throughput analysis of a large class of channel access protocols, including ALOHA, CSMA and Conservative-BTMA (C-BTMA), was presented and analyzed. This work constituted a major advance since it enabled the analysis of general topologies and traffic patterns. However, the model was restricted to the case of zero propagation delay, and did not model the effect of buffering of packets by store-and-forward repeaters, and hence it was unable to give any information about packet delay. In [15] the buffering of packets by repeaters was modelled, but only the slotted ALOHA protocol with a maximum of three buffers per repeater was considered. The difficulty in dealing with the general problem analytically, and the limitations of the analytic models so far devised, have motivated us to write a general purpose simulation program that would enable the understanding of the performance of multihop packet radio networks, without major restriction.

In this report we focus on multihop networks that have a regular structure and balanced

traffic flow. This simplifies matters by greatly reducing the number of parameters we need to consider, since all nodes perform in a statistically identical manner. We examine the effect of transmission scheduling rate, the ratio of propagation delay to packet length, and to some extent network access flow control on throughput and delay performance, and we compare the performance of various channel access schemes; namely, ALOHA, CSMA, CDMA, BTMA, and a new (idealistic) scheme referred to as Coded Activity Signalling Multiple Access (CASMA), introduced hereafter strictly for comparison purposes.

In the next section, we present a precise description of the various protocols considered in this study. Section 3 describes the essential variables considered in the simulation model of packet radio systems and the measures of system performance by which the protocols are evaluated. Finally, section 4 describes the numerical examples and discusses the results obtained.

2. Channel Access Protocols

In this section, we present the various channel access protocols considered in this report. We consider a network consisting of N nodes distributed over some geographical area. The connectivity of the network is specified by an $N \times N$ hearing matrix H , in which the (i, j) 'th element h_{ij} is 1 if node j hears node i , and zero otherwise. (We let $h_{ii} = 1, \forall i$). Each nonzero element $h_{ij}, (i \neq j)$ of the hearing matrix corresponds to a directed radio link in the network from node i to node j , and vice versa. Alternatively, a network can be represented graphically by a directed graph in which vertices represent nodes in the network, and directed edges represent one-way connectivity. For simplicity, we assume in this report that H is symmetric, and thus all edges in the graph are bidirectional. For any node i , let $\mathcal{N}(i)$ denote the set of all nodes connected to it including itself. Let $\mathcal{N}^*(i) \triangleq \mathcal{N}(i) - i$. The elements of $\mathcal{N}^*(i)$ are called neighbors of i . For a collection of nodes

A , we define $\mathcal{N}(A)$ to be

$$\mathcal{N}(A) \triangleq \bigcup_{i \in A} \mathcal{N}(i).$$

We let $\mathcal{N}^2(A) \triangleq \mathcal{N}(\mathcal{N}(A))$, and $\langle i, j \rangle$ denote a transmission from node i to node j (assuming $h_{i,j} = 1$). Given transmission $\langle i, j \rangle$, a node k is said to be hidden with respect to the transmitting node i if $k \in \mathcal{N}(j) - \mathcal{N}(i)$.

In the descriptions below, *capture* refers to the ability of a receiver to successfully receive a packet destined to it, in spite of the presence of other overlapping signals on the same channel. By *perfect capture*, we mean that once a receiver has begun to receive a packet, capture is achieved independent of the number of overlapping signals on the channel and their times of arrival. *Zero capture* refers to that situation in which any overlap of transmissions results in mutual destructive interference. We consider that all schemes, with the exception of CDMA, operate in a narrow band channel with zero capture. In the CDMA scheme, we assume that the channel is operating in the spread spectrum mode, (together with bit-by-bit code changing and receiver directed codes), in which case the probability of capture is high, and thus perfect capture is assumed.

For all the protocols described below, it is considered that nodes attempt transmission of their packets at discrete random points in time defined by some point process. In the event that a packet scheduled for transmission is inhibited by the operation of the protocol, or in the event that a transmitted packet is not captured, then that packet is again considered for transmission at some future point in time determined by the scheduling point process.

2.1 ALOHA

In this mode, it is assumed that a node is allowed to transmit only if it is not already transmitting, regardless of the activity in the rest of the network. In the **pure ALOHA**

version of this mode, packets are scheduled for transmission asynchronously (and independently). Clearly, this implies that the reception of a packet by a node is aborted if a packet transmission is scheduled at that node during the time of reception.

In the **Slotted ALOHA** version of this mode, the time axis is considered to be universal for all nodes and divided into equally sized slots. A node with a packet scheduled for transmission in a particular slot transmits that packet, synchronizing the start of transmission to coincide with the beginning of the slot. Note that since the slot size is fixed in advance, arbitrary distributions of packet length cannot be accommodated by this protocol. Note also that, due to the non-zero propagation delay among nodes, in order to have a universal slotted time axis, the slot size must be large enough to accommodate the packet transmission time plus a 'guard band' equal to the maximum of the propagation delays between pairs of neighboring nodes in the network.

2.2 CSMA

In this mode, it is required that a node be able to sense the presence of transmissions by its neighbors. A packet will be transmitted by a node only if that node is not already transmitting and no ongoing transmissions are sensed. In spite of carrier sensing, two factors remain which contribute to collisions. The first is the non-zero propagation delay between neighbors: given that a transmission $\langle i, j \rangle$ has been initiated, all nodes in the set $\mathcal{N}^*(i)$ are not blocked from transmitting until the transmission from node i has been sensed by them all; thus the propagation time from node i to its neighboring nodes constitutes a *vulnerable period* for the transmission $\langle i, j \rangle$ as far as transmissions from $\mathcal{N}^*(i) \cap \mathcal{N}(j)$ are concerned. The second factor is *hidden nodes*: given that a transmission $\langle i, j \rangle$ has been undertaken, all nodes in $\mathcal{N}(j) - \mathcal{N}(i)$ cannot sense the presence of $\langle i, j \rangle$, and are thus never blocked; in this case the entire packet transmission time constitutes a vulnerable period for $\langle i, j \rangle$ as far as transmissions from hidden nodes are concerned.

2.3 BTMA

The problem of collisions caused by hidden nodes can be alleviated by the use of a busy tone on a separate channel, which is emitted by a node to indicate that it is currently receiving a packet. The busy tone is then used to inhibit the receiving node's neighbors from transmitting and thereby interfering with it. Several variants of BTMA exist depending on which set of nodes transmit a busy tone in any given situation, as outlined below.

a. Conservative BTMA (C-BTMA): Whenever a node senses a transmission, it emits a busy tone regardless of whether it is the immediate destination or not. Then any node that wishes to transmit is allowed to do so only if it is not already transmitting and no busy tone is sensed. Given that a transmission $\langle i, j \rangle$ has been undertaken, then after a one-hop propagation delay, all nodes in the set $\mathcal{N}^*(i)$ sense the presence of $\langle i, j \rangle$, and emit a busy tone. After another propagation delay, busy tone is detected by all nodes in $\mathcal{N}^2(i) - \mathcal{N}(i)$. Thus, for the transmission $\langle i, j \rangle$, a one-hop propagation delay constitutes a vulnerable period as far as transmissions from nodes in $\mathcal{N}^*(i) \cap \mathcal{N}(j)$ are concerned, while a two-hop propagation delay constitutes a vulnerable period as far as transmissions from nodes in $\mathcal{N}(j) - \mathcal{N}(i)$ are concerned. Note that, if the propagation delay between nodes is zero, then C-BTMA is collision free.

b. Idealistic BTMA (I-BTMA): This scheme is similar to C-BTMA except that whenever a node senses a transmission, it emits a busy tone only if it is the immediate destination. Clearly, without prior knowledge, a node may not know if a particular transmission is destined to it or not, hence the name idealistic. It is considered here for comparison purposes. Given that transmission $\langle i, j \rangle$ has been undertaken, then after a vulnerable period equal to a two-hop propagation delay, all nodes in the set $\mathcal{N}^*(j)$ are blocked from transmitting. Alternatively, one may additionally make use of carrier sensing. This way, all nodes in $\mathcal{N}^*(i)$ (which includes $\mathcal{N}^*(i) \cap \mathcal{N}(j)$) are blocked after a vulnerable period of

only a one-hop propagation time, while nodes in the set $\mathcal{N}(j) - \mathcal{N}(i)$ are blocked after a vulnerable period equal to a two-hop propagation time. In this work, only the latter scheme is studied.

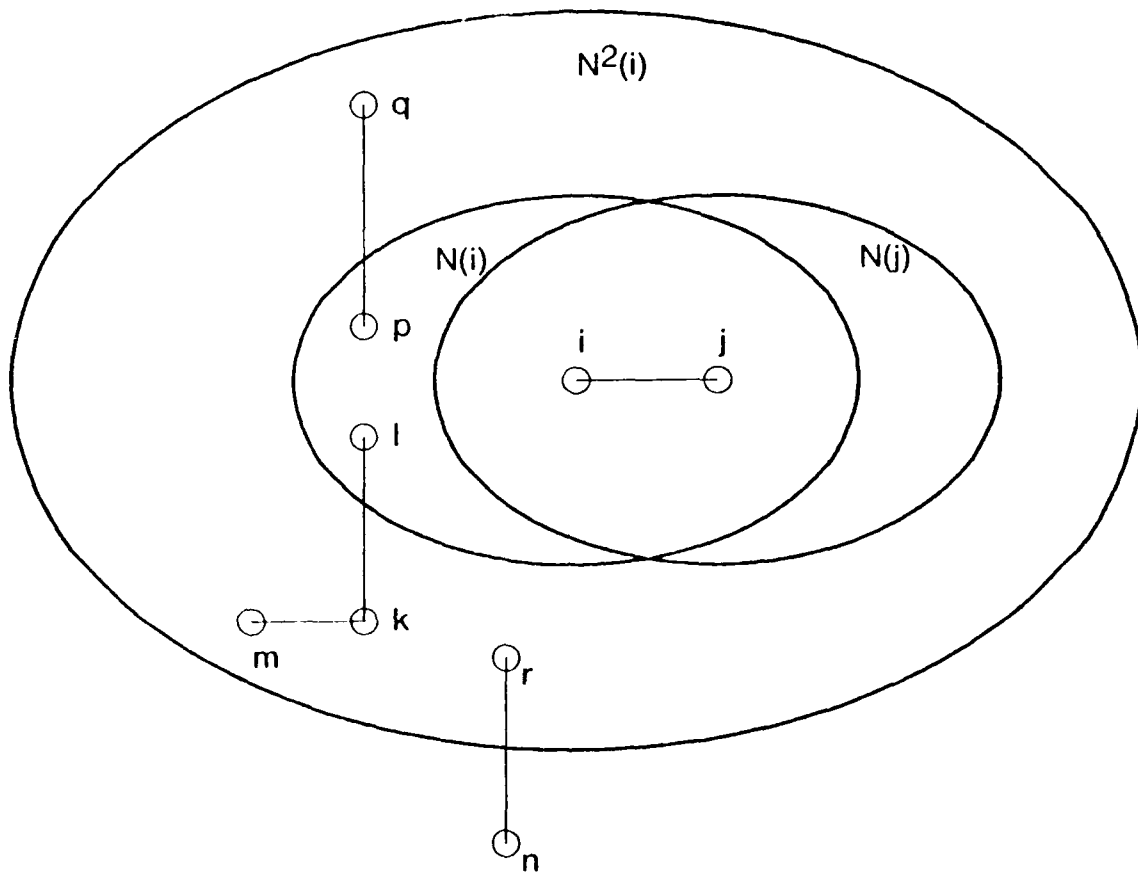


Fig. 1 Example of a set of transmissions in a multihop packet radio network.

We now examine in more detail some of the ramifications of these two BTMA schemes. Assume for the purpose of this discussion, that the propagation delay is zero. Consider the following situation depicted in figure 1. Let node i be transmitting to node j and let all other nodes be silent. Assume that a packet from node $k \in \mathcal{N}^2(i) - [\mathcal{N}(i) \cup \mathcal{N}(j)]$ destined to node $m \in \mathcal{N}^2(i) - \mathcal{N}(i)$ is scheduled for transmission during the transmission $\langle i, j \rangle$. In C-BTMA the transmission $\langle k, m \rangle$ is blocked, while in I-BTMA it results

in a successful transmission.

On the other hand, in I-BTMA (and CSMA for that matter) it is possible to allow a transmission to take place that will be unsuccessful, and whose presence may block a number of other potentially successful transmissions, while in C-BTMA, the former transmission would be inhibited by the protocol, allowing the later potentially successful transmissions to then take place. For example, referring to figure 1, consider now that a packet from node k destined to node $l \in \mathcal{N}(i)$ is scheduled for transmission during the transmission time of $\langle i, j \rangle$. Furthermore, let $n \notin \mathcal{N}^2(i)$ and $r \in \mathcal{N}^2(i) - \mathcal{N}(i)$, and consider a transmission $\langle n, r \rangle$ to be scheduled at some point in time during the transmission time of $\langle k, l \rangle$. In I-BTMA, the transmission $\langle k, l \rangle$ is not blocked, but is unsuccessful; the transmission $\langle n, r \rangle$ is blocked if $n \in \mathcal{N}(k)$; the transmission $\langle n, r \rangle$ is unblocked but unsuccessful if $n \notin \mathcal{N}(k)$ and $r \in \mathcal{N}(k)$. In the latter case n 's unsuccessful transmission will have blocking and interfering effects on its neighbors similar to those of node k 's transmission. However, in C-BTMA, the transmission $\langle k, l \rangle$ is blocked and the transmission $\langle n, r \rangle$ is successful. It is not clear which of the effects outlined above would predominate in a given situation, and hence we resort to simulation to compare the different schemes.

c. Hybrid BTMA (H-BTMA): In I-BTMA, we assume hypothetically that as soon as a node receives a packet it knows immediately whether or not that packet is destined to it. In practice this information is obtained from the packet header. Assuming that the packet header is processed as soon as it is received and before the entire packet is received, the time at which a node can first determine whether or not it is the intended immediate destination for a particular packet reception is at the end of the processing of the packet header. In H-BTMA, a node operates as in C-BTMA until the header is processed, upon which time it operates as in I-BTMA. (Alternatively one may conceive of a scheme in which the node operates as in CSMA until the header is processed prior to switching to

I-BTMA. We consider only the former scheme in this study.)

2.4 CASMA

As discussed above, depending on the particular situation, both C-BTMA and I-BTMA have their shortcomings. In order to see how good a performance is achievable using random multiaccess protocols in multihop packet radio networks, we consider the following hypothetical CASMA protocol: a node is allowed to transmit only if it is not already transmitting, it is not already receiving a packet destined to it, no neighbor is receiving a packet destined to that neighbor, and its immediate destination is currently neither transmitting nor sensing carrier.

Clearly, as with I-BTMA, without prior knowledge a node may not know if a particular transmission is destined to it or not. Hence, in practice, a hybrid form of this protocol would be used. In such a hybrid scheme, before the header is processed the protocol operates in one mode (such as C-BTMA), and after the header is processed it operates in the CASMA mode. In this study, in order to obtain a bound on performance, we consider only the idealistic case where prior knowledge of the immediate destination is assumed. We assume that the activity signalling functions required by this protocol are implemented by means of a busy tone emitted by a node when it is receiving a packet destined to it, and the use of a carrier sense tone emitted by a node when it is transmitting or detecting carrier due to a packet transmission not destined to it. In addition, it is required that the carrier sense tone be coded so that it allows unique identification of the node emitting it.

The essence of CASMA is that, given the state of the network in terms of ongoing transmissions, a scheduled transmission in the network is allowed to take place only if it has a high probability of not interfering with an ongoing transmission; furthermore, once allowed, the transmission has a high probability of success since all other nodes operate under the same protocol. (If the propagation delay is zero, then both probabilities would

be unity.) Given that transmission $\langle i, j \rangle$ has been undertaken, then after a vulnerable period equal to a two-hop propagation delay, all nodes in the set $\mathcal{N}^*(j)$ are blocked and all transmissions destined to nodes in $\mathcal{N}(i)$ are inhibited.

To illustrate the benefits gained by this scheme, we reexamine the various situations considered above and depicted in figure 1. Let nodes i, j, k, l, n and r , and the scheduled transmissions among them be as defined above. Transmission $\langle k, l \rangle$ is inhibited due to l 's carrier sense tone, and thus transmission $\langle n, r \rangle$ can take place successfully (as in C-BTMA). Consider, on the other hand, transmission $\langle k, m \rangle$; $\langle k, m \rangle$ can take place successfully in CASMA, while it is blocked in C-BTMA; as for transmission $\langle n, r \rangle$, in CASMA it is inhibited if $r \in \mathcal{N}(k)$, but is successful if $r \notin \mathcal{N}(k)$. Moreover, given an on-going transmission from node i to node j and all other nodes silent, any node $p \in \mathcal{N}(i) - \mathcal{N}(j)$ with a packet scheduled for transmission to a node $q \in \mathcal{N}^2(i) - \mathcal{N}(i)$ during the transmission $\langle i, j \rangle$ will transmit successfully in CASMA; (note that node p is blocked in CSMA, C-BTMA, as well as I-BTMA). Thus the action taken in CASMA in each situation is expected to lead to a performance that is superior to both that of I-BTMA and C-BTMA. (We thus consider CASMA to provide an upper bound on the performance of the other schemes.)

2.5 CDMA

In this case we assume that spread spectrum operation is in effect. Each node is assigned a unique code for reception. Nodes wishing to transmit to a particular node must use the code assigned to that node. A receiver that is idle 'locks onto' a packet with the appropriate code by correctly receiving a preamble appended in front of the transmitted packet. When reception of a packet is completed, the receiver becomes free again until another packet with the correct preamble is received. A node is allowed to transmit only if it is neither transmitting nor 'locked on'.

This is not the only way to make use of spread spectrum modulation. A number of access schemes that operate in the CDMA mode have recently been proposed and analyzed, such as Destination Code Sensing Multiple Access [13], and Channel Load Sensing [16]. In the former access scheme, the source node monitors the channel for activity using the code assigned to the destination of the packet being considered for transmission, prior to attempting to transmit. Transmission is inhibited if such activity is detected. In the latter scheme, the source node is assumed to be able to sense the number of transmissions on the channel. Transmission is inhibited if the node is either transmitting, 'locked on', or if the number of transmissions sensed exceeds a predetermined threshold. In this study, for the sake of simplicity, we consider that the presence of any number of overlapping transmissions on the channel does not affect the captured packet's reception. (Thus perfect capture is assumed). We also assume that preambles are of zero length.

3. The Simulation Model and the Measures of System Performance.

In this section we describe the constituent variables of packet radio networks that have been considered in this simulation study. We also describe the traffic model used for packet generation, the packet scheduling algorithm, and the performance measures used in evaluating the access schemes.

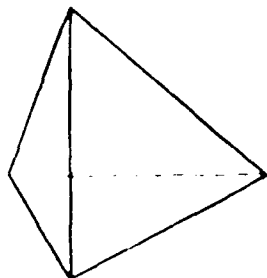
It should be kept in mind that our primary aim in this report is to investigate the performance of various channel access policies. Hence we have made certain simplifying assumptions, as a first step in achieving our goal, in order to keep the simulation task manageable. These assumptions are thought to have little impact on the comparative evaluation of the access schemes. In particular, we have considered networks in which the structure, traffic requirement and operational algorithms are such that all nodes perform

in a statistically identical manner and all links carry the same traffic load. (Many of these assumptions will be relaxed in future studies and investigated in more detail.)

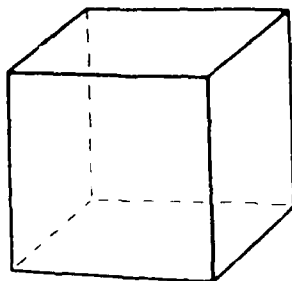
3.1 Network Structure and Operational Protocols

Two classes of regular topologies are considered: regular (Platonic) solids and ring topologies. (See figure 2). The regular solids are symmetric three-dimensional structures with the number of nodes N varying from 4 to 20, and nodal degree, denoted by d , varying from 3 to 5. Although these structures are not typical of packet radio networks, they are chosen so as to represent planar networks of different nodal degree that are totally symmetric and that do not present special boundary conditions. For cases where the number of nodes N is not too small, regular solids are thought to approximate fairly closely, with a finite number of nodes, an infinite regular planar topology. Ring topologies with $d = 2$ (referred to as simple rings) approximate a linear string of repeaters in a packet radio network. In this report, we also consider 'multiconnected' rings with nodal degree $d > 2$, as shown in figure 2. Multiconnected rings represent a string of repeaters where the transmission radius extends beyond the nearest neighbors. They are simple topologies in which the number of nodes N and the nodal degree d can to a large extent be arbitrarily chosen, thus enabling us to experiment with the effects of N and d on the performance of the channel access schemes. In all regular solid topologies, the same propagation delay exists between all pairs of adjacent nodes. This is also assumed to be the case in the simulation model for ring topologies (simple and multiconnected).

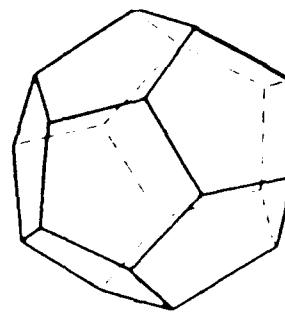
It is assumed that unlimited buffer resources are available at each node, with separate queues for each outgoing link. We assume that the acceptance rate of destinations is unlimited, and thus we do not consider end-to-end flow control schemes. We do consider, however, network access flow control, and make use of a particular scheme referred to as the input buffer limit (IBL) scheme [17]. Such a scheme restricts network access for new



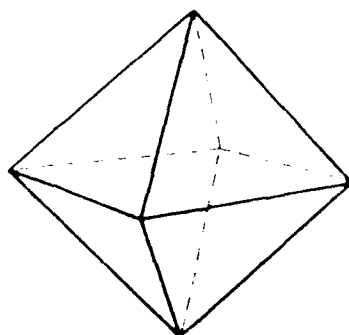
TETRAHEDRON
 $N = 4$ $d = 3$



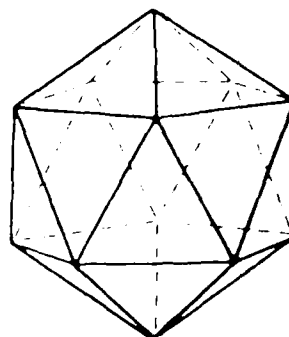
CUBE
 $N = 8$ $d = 3$



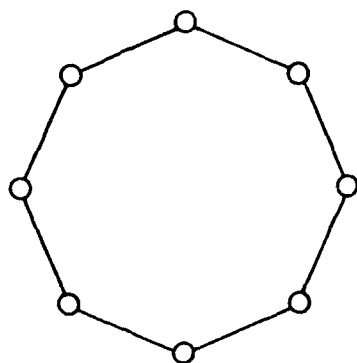
DODECAHEDRON
 $N = 20$ $d = 3$



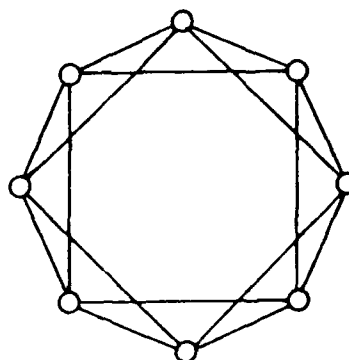
OCTAHEDRON
 $N = 6$ $d = 4$



ICOSAHEDRON
 $N = 12$ $d = 5$



RING
 $d = 2$



MULTICONNECTED RING
 $d = 4$

Fig. 2 Network topologies.

packets attempting to join a given queue by causing rejection of such new packets whenever the total number of packets (new and in transit) in that queue exceeds a certain number m . An alternative scheme, also considered here, consists of rejecting new packets when the total number of such packets exceeds a certain number m' .

The routing algorithm used is a static shortest path scheme, with the path length based on number of hops. Where several shortest paths between a source-destination pair exist, all such paths are selected with equal likelihood.

We assume that acknowledgements are instantaneous and for free; that is, the sender learns of the success or failure of its transmission as soon as the packet has been completely received at the intended immediate destination, and the acquisition of this knowledge is assumed not to require any communication bandwidth*.

3.2 Traffic Model

We define the network input traffic requirement by the matrix $[\gamma_{ij}]$, where γ_{ij} , $i \neq j$, is the average number of packets per unit time offered at node i and ultimately destined for j . (We let $\gamma_{ii} = 0$, $\forall i$). The total traffic offered to the network is denoted by γ and is given by $\sum_{i=1}^N \sum_{j=1}^N \gamma_{ij}$. In this study, we consider two types of input traffic matrices, namely, the *uniform* traffic matrix in which γ_{ij} is constant for all pairs of nodes, and equal to $\gamma/N(N-1)$, and the *neighbors-only* traffic matrix in which $\gamma_{ij} = \gamma/dN$ if $h_{ij} = 1$, $i \neq j$, and $\gamma_{ij} = 0$ otherwise. Provided that the routing algorithm described above is used, the internal traffic is balanced throughout the network; i.e., the link traffic is the same for all links.

*It is believed that this assumption would not have a major effect on the comparative evaluation of the various schemes. It may however affect their absolute performance. There are several ways of implementing hop-by-hop acknowledgements in packet radio networks [6,18]. These will be evaluated in a separate study. The effect of acknowledgement traffic on the performance of the various schemes will then be identified.

The generation of packets at a source node forms a random process considered here to be Poisson. We assume that packets are of constant length. Thus the transmission time of a packet is also a constant. We define a to be the ratio of the propagation delay to packet transmission time.

3.3 Scheduling of Packet Transmissions

It is assumed that there is a single transmitter per node. The transmitter is shared among the queues of the node, and a First Come First Served (FCFS) service discipline is utilized at each queue. Associated with each node of the network, there is also a random point process which defines the points in time when transmissions may be attempted. These points are referred to as *scheduling points*. At each scheduling point, the node executes the following algorithm:

- (i) If the transmitter is already engaged in a transmission, or if all the queues of a node are empty, then the scheduling point is ignored.
- (ii) Otherwise (the transmitter is free and one or more queues are not empty), the packet at the head of some non-empty queue is considered for transmission. The selection of the non-empty queue, whose head is to be considered for transmission, is random according to a uniform distribution. Clearly, actual transmission of the packet may or may not take place depending on the state of the network and the blocking property of the particular channel access protocol in use:
 - a) If the attempted transmission is inhibited, then the scheduling point is lost.
 - b) Otherwise the transmission is undertaken.

Once the packet has been transmitted successfully, then it is deleted from the head of its queue. In this study, the scheduling point process for node i is assumed to be Poisson (with rate G_i ; scheduling points per packet transmission time) for the ALOHA,

CSMA, BTMA, CASMA and CDMA protocols, and Bernoulli (with probability G_i of transmitting in a slot) for the slotted ALOHA protocol.

3.4 Measures of System Performance

There are essentially two measures of performance which we consider in this study, namely network throughput and packet delay. We define the throughput matrix $[S_{ij}]$ so that its (i, j) 'th element S_{ij} , $1 \leq i, j \leq N$, is the average number of successful receptions at destination node j of packets that originated at source node i , per packet transmission time. The total end-to-end network throughput is

$$S = \sum_{i=1}^N \sum_{j=1}^N S_{ij}.$$

Another measure of throughput performance of interest in this study is the nodal throughput denoted by s_i , $1 \leq i \leq N$, where s_i is the average number of successful transmissions by node i to all its neighbors, per packet transmission time.

We define the delay matrix $[\delta_{ij}]$ so that its (i, j) 'th element δ_{ij} specifies the average time a packet from source node i destined to ultimate destination node j spends in the system from the time it is accepted at node i until it is finally successfully received at node j , normalized to the packet transmission time. If, due to the input buffer limit control scheme, a newly generated packet is not accepted at a source node, then it is considered lost and does not contribute to the measured delay. The average packet delay over the entire network is given by

$$D = \sum_{i=1}^N \sum_{j=1}^N \frac{S_{ij}}{S} \delta_{ij}.$$

We also consider the distribution of buffer occupancy per queue. For a given queue i , let L_i denote the number of new and transit packets in the queue in steady state.

Let $q \in [0, 1]$. We define a buffer occupancy q th quantile to be an integer n_q such that $\Pr[L_i > n_q] \leq 1 - q$.

4. Numerical Results

Consider a packet radio network according to the model described in section 3. The topology may be any of the regular structures introduced with the exception of multiconnected rings. The latter will be examined in more detail in subsection 4.3. Due to the assumptions of uniformity in the offered input traffic matrix, and the balanced shortest path routing, all nodes behave in a statistically identical manner. Hence we may consider all nodal scheduling rates to have the same value denoted by G . Moreover, all nodes have equal nodal throughput s , all source-destination pairs have equal end-to-end throughput, (which is $S/N(N-1)$ in the case of the uniform traffic matrix, and $S/Nd = s/d$ in the case of the neighbors-only traffic matrix), and all paths of equal length have identical end-to-end average packet delay. Note that $S = Ns/\bar{n}$, where \bar{n} denotes the mean number of hops between a source and a destination.

Let $S(\gamma, m, G)$ denote the total end-to-end throughput for γ , m , and G . Assume $m = \infty$ (i.e., no external packet is ever rejected), and heavy-traffic conditions (i.e., $\gamma = \infty$). Under these conditions, given the (regular) network structures under consideration and the random nature of the access schemes, it is guaranteed that all queues in the network will always be non-empty. Since the number of nodes in the network is finite and no incoming transit packet at a node is ever rejected (due to the infinite buffer assumption), it is intuitively clear that the mean service time X for a packet at the head of a queue, (defined as the expected time from when a packet moves to the head of the queue until it is successfully transmitted to its immediate destination) is finite and constant over time, and entirely determined by the network topology, the access scheme, and the scheduling

rate G . This also means that the link throughput (i.e., the fraction of time that a link is engaged in successful transmissions) is nonzero and equal to $1/X$ packets per second. Let $C(G) \triangleq \lim_{\gamma \rightarrow \infty} S(\gamma, \infty, G)$. $C(G)$ is the total end-to-end network throughput under heavy-traffic for the scheduling rate G , and is called the *capacity* of the network at scheduling rate G . We define nodal capacity in a similar fashion. Let $s(\gamma, m, G)$ denote the nodal throughput for γ , m and G , and define the nodal capacity as $c(G) \triangleq \lim_{\gamma \rightarrow \infty} s(\gamma, \infty, G)$. As with the network and nodal throughput, $C(G)$ and $c(G)$ are related according to $C(G) = Nc(G)/\bar{n}$. With $m = \infty$, it is clear that for $\gamma \leq C(G)$ we must have $S(\gamma, \infty, G) = \gamma$, and for $\gamma > C(G)$, $S(\gamma, \infty, G) = C(G)$. Such expectations are entirely confirmed by simulation, as will be shown in the following subsection. Note that $c(G)$ is the same for both traffic matrices considered in this study, while $C(G)$ differs due to the differences in \bar{n} .

As a first step in the discussion of the numerical results, a representative example network consisting of the simple six node ring topology together with the C-BTMA access scheme is selected for an in-depth study with the purpose of identifying explicitly the effect of the scheduling rate and the input flow control on throughput and delay performance. As all other network topology and access scheme combinations (again with the exception of multiconnected rings) exhibit similar behaviour, we limit the remainder of the section to a comparison of the performance of the various access schemes in the different networks, on the basis of their capacity and throughput-delay characteristics.

4.1 A Representative Example

The example considered here is a simple six node ring with $a = 0.01$ operating under C-BTMA with a uniform offered traffic matrix and balanced shortest path routing. In figure 3 we plot the network throughput $S(\gamma, m, G)$ versus γ with m set to 50 (a somewhat arbitrary but large value). The difference between the simulation points and the expected

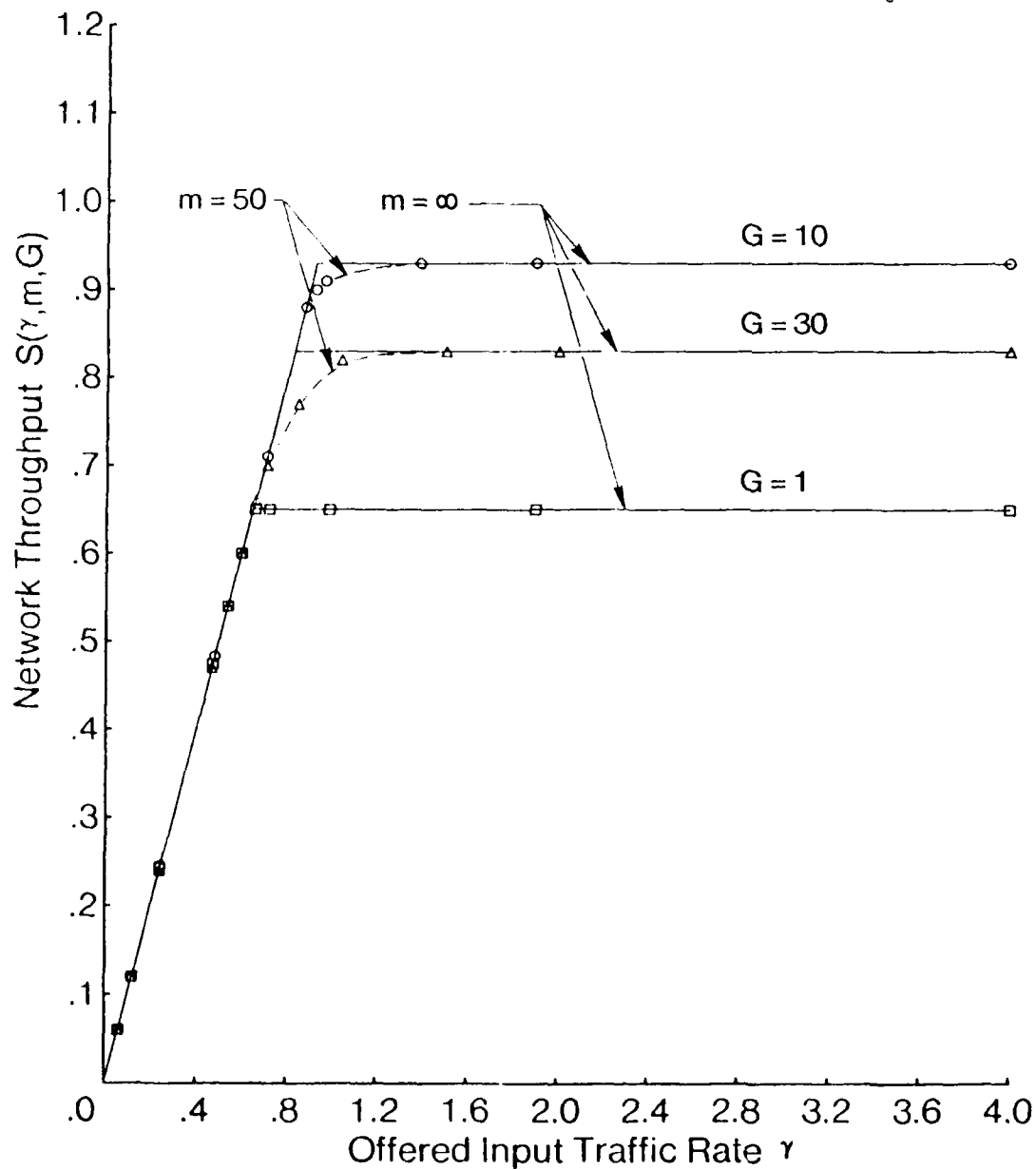


Fig. 3 Network throughput versus offered input traffic rate in a simple six node ring network, under the C-BTMA protocol, with a uniform traffic matrix and $\alpha = 0.01$.

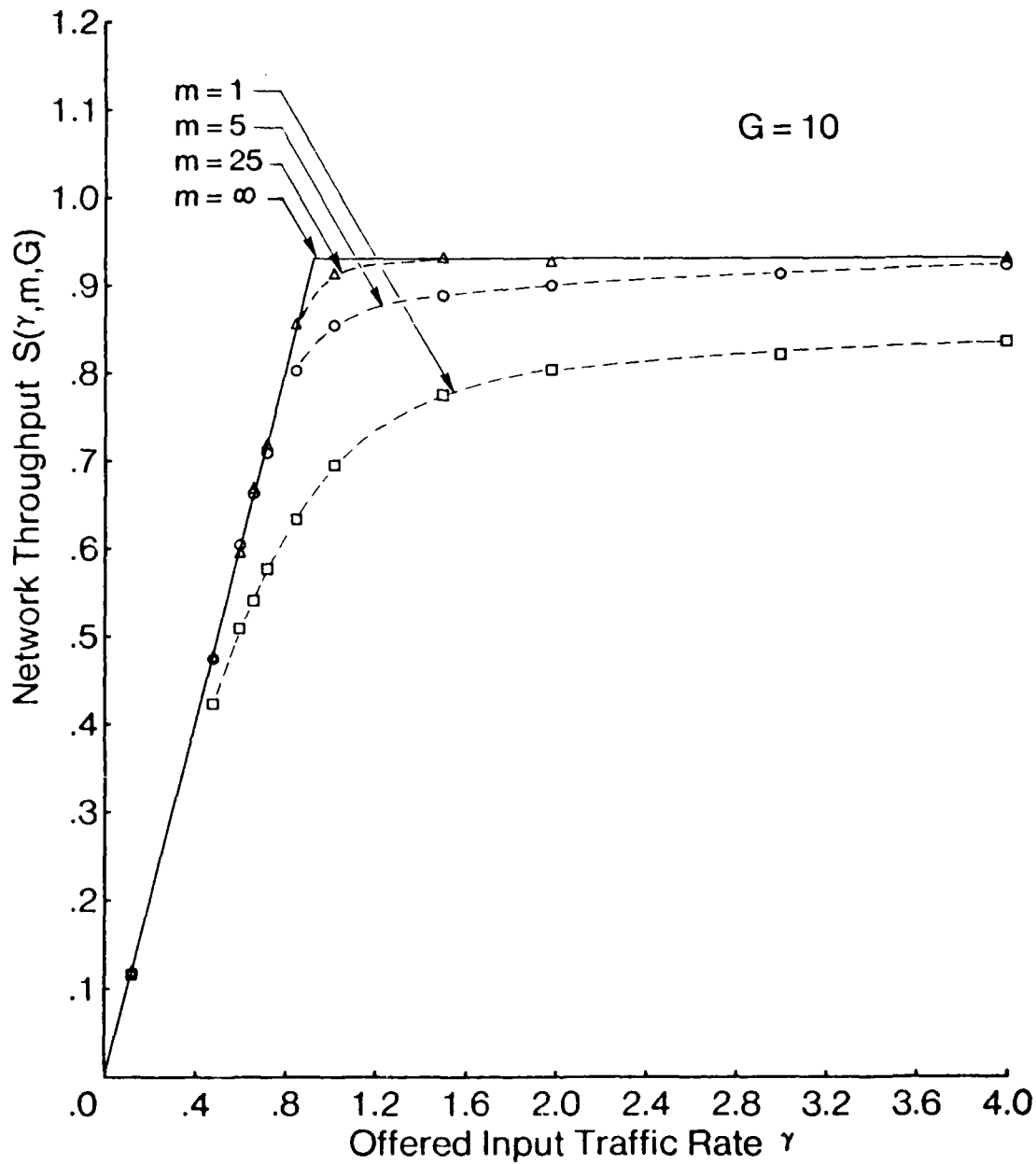


Fig. 4 Network throughput versus offered input traffic rate, for various input buffer limits m , (with rejection of new packets when new and transit packets exceed m), in a simple six node ring network under the C-BTMA protocol, with a uniform traffic matrix, $a = 0.01$ and $G = 10$.

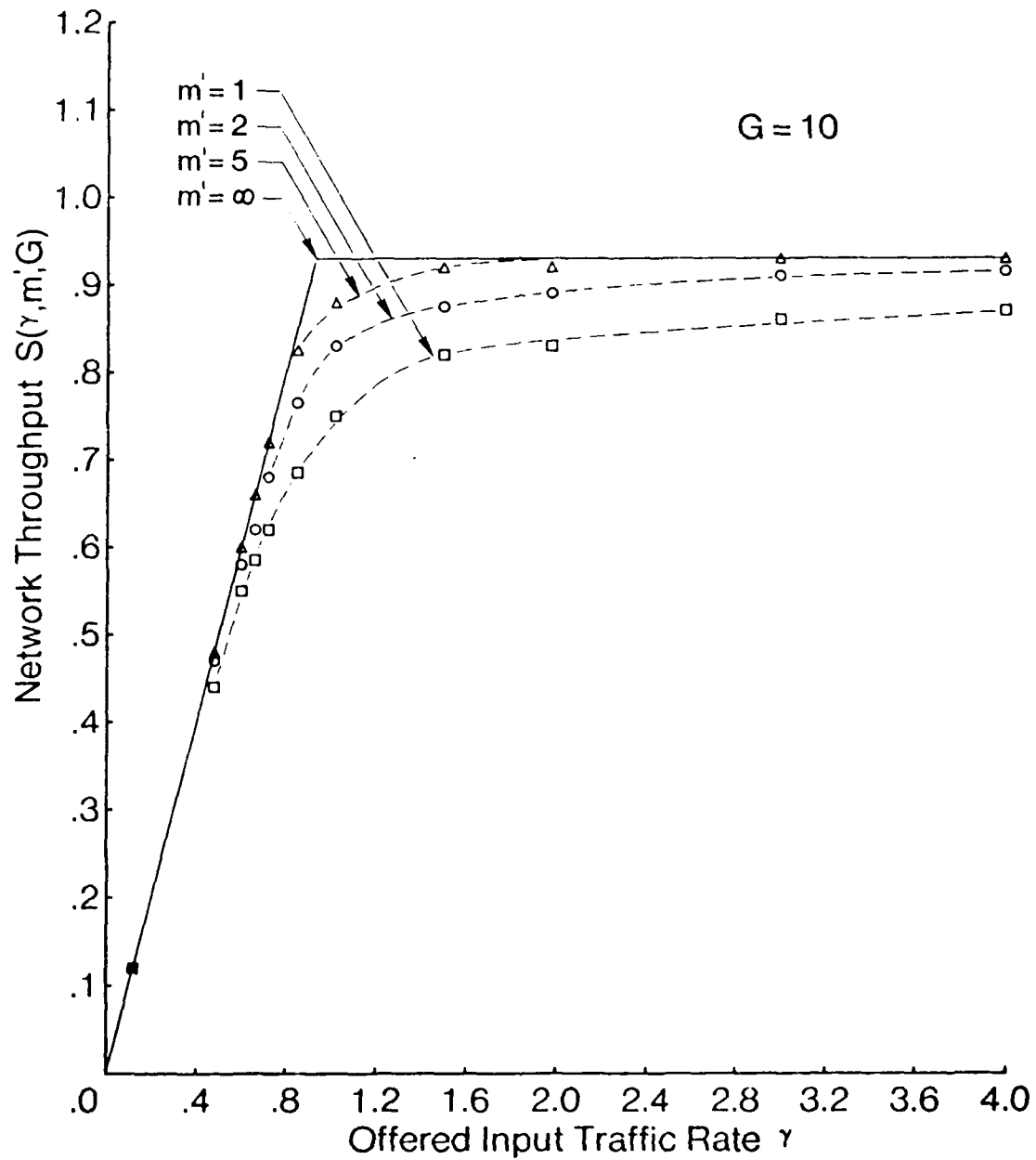


Fig. 5 Network throughput versus offered input traffic rate, for various input buffer limits m' , (with rejection of new packets when m' new packets are already present), in a simple six node ring network under the C-BTMA protocol, with a uniform traffic matrix, $a = 0.01$ and $G = 10$.

curves in the vicinity of $\gamma = C(G)$ is due to the finite value used for m , which causes some new packets to be rejected. Indeed, the probability $P_b(\gamma, m, G)$ of an input packet being rejected is nonzero for $m < \infty$, and increases for decreasing values of m . The larger m is, the closer the simulation points are to the expected curve ($m = \infty$) as can be seen in figure 4. We note, however, that regardless of the value of m , we have

$$\lim_{\gamma \rightarrow \infty} S(\gamma, m, G) = C(G).$$

The results shown in figures 3 and 4 correspond to the IBL scheme where a new packet is rejected if the total number of packets in the queue (new and transit) exceeds m . The alternative scheme (as described in section 3.1) considers that a new packet offered to a queue is rejected if the number of new packets in that queue reaches m' . (Transit packets are again not affected, since we have assumed infinite buffers at each queue). In figure 5 we show S versus γ for various values of m' . For equal values of m and m' , this IBL control scheme clearly achieves a higher throughput than the former scheme, since the blocking probability is smaller; in all other respects the behaviour is the same. We also have

$$\lim_{\gamma \rightarrow \infty} S(\gamma, m', G) = C(G)$$

where $C(G)$ is the same in both IBL schemes. In the sequel we shall consider only the first IBL control scheme.

The scheduling rate G has an important effect on the network capacity $C(G)$. The latter is maximized for a particular value of G , denoted by G^* . $C(G^*)$ is referred to as the *optimum network capacity*. The effect of G is illustrated in figure 6 where we plot $C(G)$ versus G . To the left of G^* , $C(G)$ is limited by the small value of G (and hence the large intervals between scheduling points); to the right of G^* , $C(G)$ is limited by an increase in the rate of collisions. (We note here that the determination of $C(G)$ by simulation is obtained by guaranteeing that all queues are always non-empty, which is simply achieved

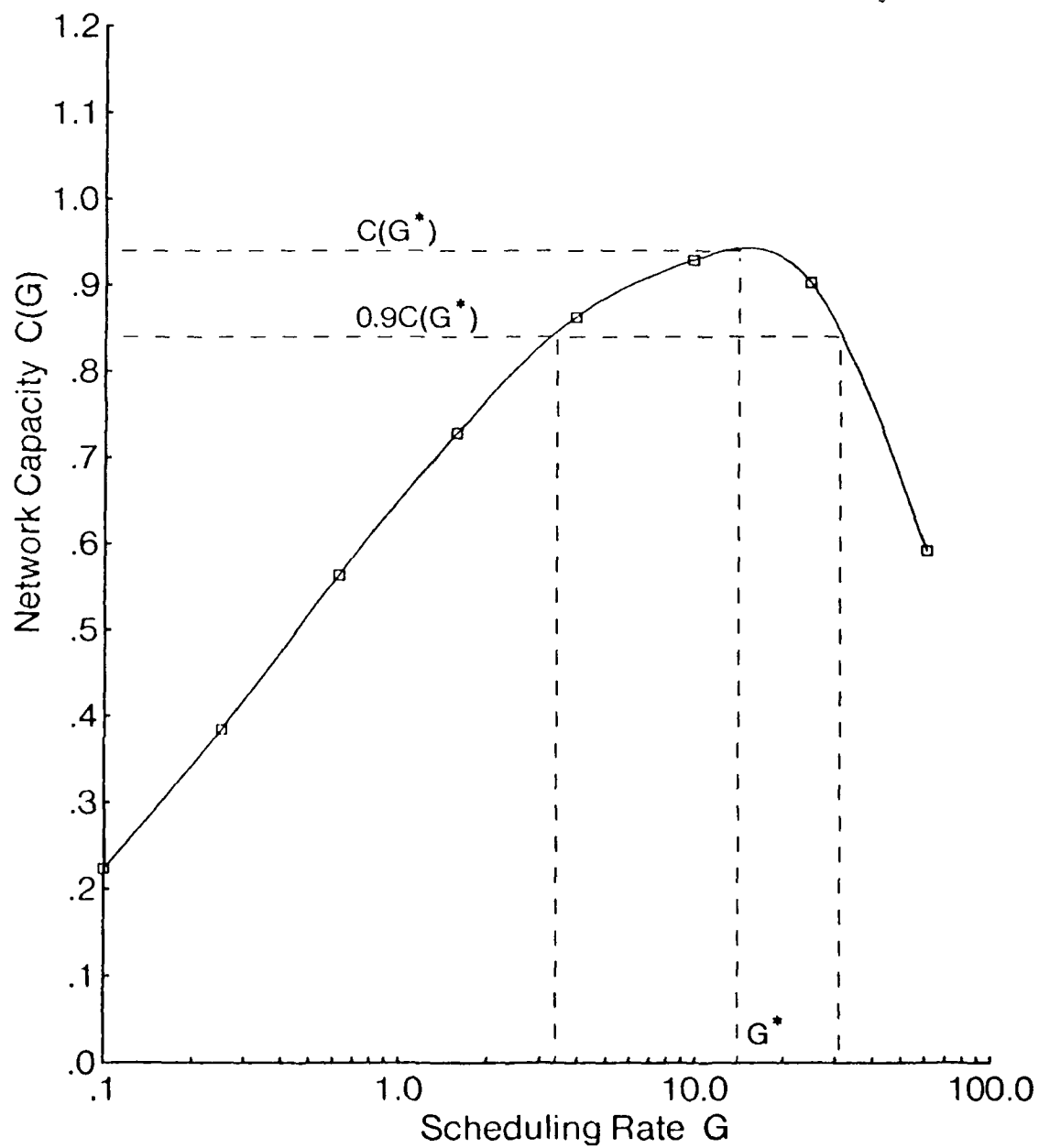


Fig. 6 Network capacity versus scheduling rate in a simple six node ring network, under the C-BTMA protocol, with a uniform traffic matrix and $\alpha = 0.01$.

by considering the first IBL scheme with $m = 1$ and $\gamma = \infty$). Note that the variation of $C(G)$ with respect to G is small in the vicinity of G^* implying a degree of insensitivity to G . For instance, we see in figure 6 that $C(G) \geq 0.9C(G^*)$ for $0.2G^* \leq G \leq 2G^*$.

We now examine the network packet delay D . As defined in section 3.4, D is the average delay of a packet from when it is admitted to the network, until it is delivered to its ultimate destination. It is a function of γ, m and G , which we denote by $D(\gamma, m, G)$. In figure 7 we plot $D(\gamma, m, G)$ versus γ for various values of m and $G = 10$. Recall that when m is finite, all rejected (external) packets do not contribute to the calculation of $D(\gamma, m, G)$. Accordingly, it is not surprising to see the network delay increase with γ , but level off at a limit which is a function of m . In practice, data packets that are blocked at the network input are stored by the host attached to the local PRU, (thus undergoing a delay), and are resubmitted at a later time. Thus a more reasonable measure of the total packet delay is obtained for a value of $m = \infty$, where new packets are accepted without limitation. As expected, for $m = \infty$, the delay becomes unbounded as $\gamma \rightarrow C(G)$.

The case $\gamma = \infty, m = 1$ is an interesting one to examine more closely. By setting $m = 1$, given the IBL scheme under consideration, no new packet is admitted to a queue until that queue empties. Furthermore as soon as the queue empties, a new external arrival is created ($\gamma = \infty$). This represents the situation where traffic is heavy, (hosts have infinite queues of packets to be offered to the network,) but priority service is given to transit packets in a first-come-first-served (FCFS) order. $D(\infty, 1, G)$ represents the network delay of packets that are admitted to the network. In figure 8, we plot the network delay for 1-, 2- and 3-hop traffic, as well as the average delay over all traffic ($D(\infty, 1, \gamma)$) versus $C(G)$. Observe that 1-hop traffic does not pass through intermediate nodes, while 2-hop traffic is forwarded through 1 intermediate queue, and 3-hop traffic through 2 intermediate queues. As before, let the service time of a packet be the time from when the packet first reaches the head of its queue, until the time it is successfully

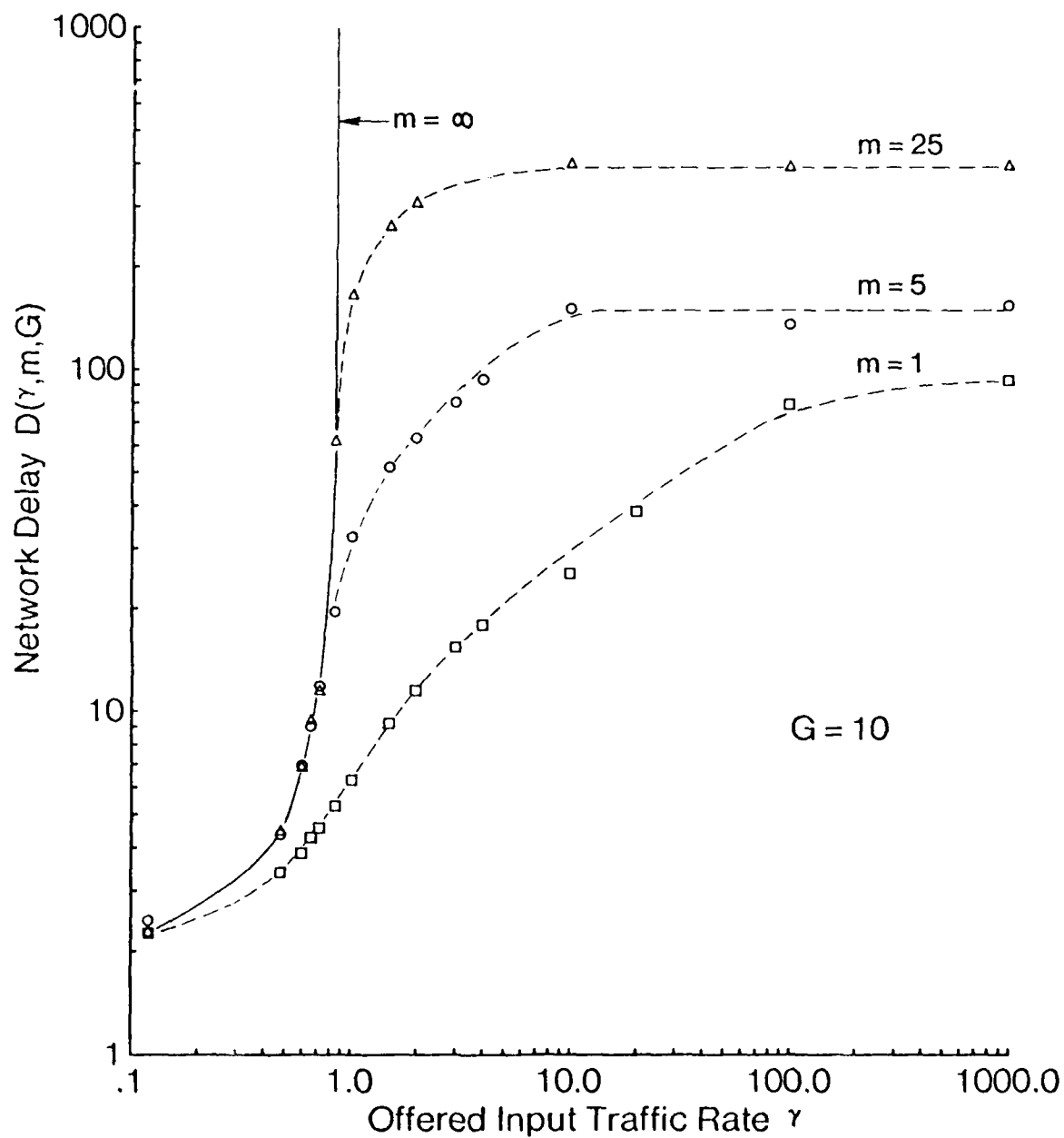


Fig. 7 Network delay versus offered input traffic rate, for various input buffer limits, in a simple six node ring network under the C-BTMA protocol, with a uniform traffic matrix, $\alpha = 0.01$ and $G = 10$.

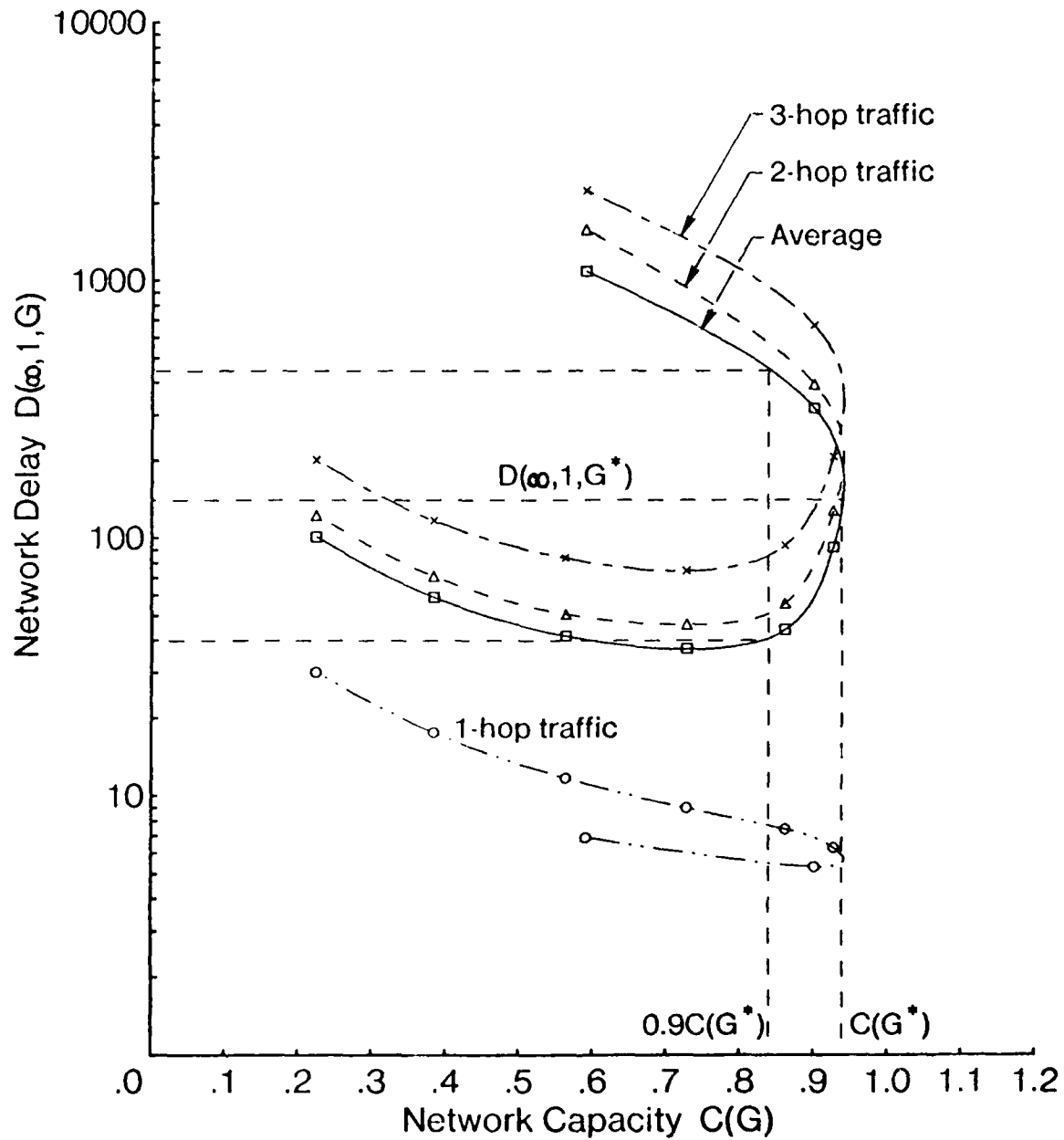


Fig. 8 Network delay versus network capacity in a simple six node ring network, under the C-BTMA protocol, with a uniform traffic matrix, $a = 0.01$, $\gamma = \infty$ and $m = 1$.

received by its intended immediate destination. Then, the 1-hop delay consists of 1 service time, the 2-hop delay consists of 2 service times and 1 queueing delay, and the 3-hop delay consists of 3 service times and 2 queueing delays. $D(\infty, 1, G)$ is observed to first decrease with $C(G)$, and then increase as $C(G)$ increases. The explanation for this is that low values of $C(G)$ correspond to low values of G , and for low values of G packets remain at the server for long periods of time due to large scheduling delays. However, as G and $C(G)$ increase, the scheduling delay decreases, which tends to decrease the network delay. As G increases further however, the system begins to operate close to capacity, and hence queueing delays begin to increase significantly, and in addition, the probability of collision and hence retransmission also increases, causing a sharp increase in network delay, and ultimately a reduction in $C(G)$. We observe that in the vicinity of network capacity $C(G^*)$, network delay is more sensitive to the scheduling rate than is the case for throughput; (an effect similar to that observed for fully connected networks [20]): we see that approximately $0.4D(\infty, 1, G^*) \leq D(\infty, 1, G) \leq 4D(\infty, 1, G^*)$ for $C(G) \geq 0.9G^*$ which corresponds to $0.2G^* \leq G \leq 2G^*$.

The buffer occupancy statistics for the case of $\gamma = \infty$ and $m = 1$ represent the buffer requirement for *transit* packets, (and potentially a single external packet,) under heavy traffic conditions. In figure 9 we plot the q th quantiles of buffer occupancy n_q versus capacity $C(G)$ for different probabilities q of exceeding n_q buffers. As $C(G)$ approaches $C(G^*)$, the q th quantiles of buffer occupancy n_q increase with $C(G)$, indicating that more and more buffers are being occupied by packets in transit. The curves of figure 9 can be used as a guide for the selection of a finite transit buffer size. For example, at a throughput $S = 0.9C(G^*)$, the probability q that the buffer occupancy exceeds 20 is less than 0.001, implying that a buffer size of 20 would be a safe choice as far as achieving $0.9C(G^*)$ goes.

The previous discussion has focused on a particular access scheme (C-BTMA) and a particular topology (a simple six node ring). For other network and access scheme combi-

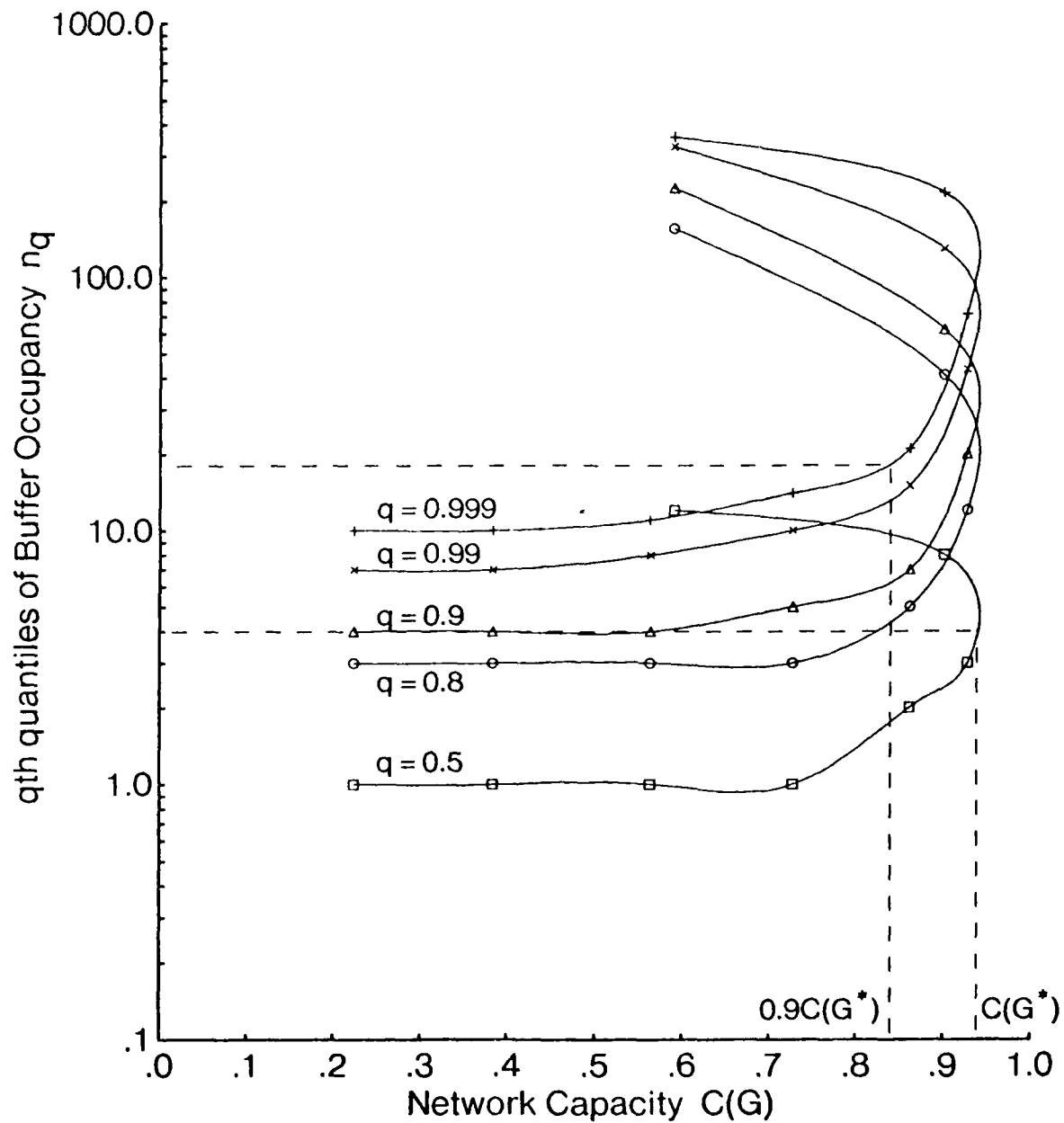


Fig. 9 q th quantiles of buffer occupancy versus network capacity in a simple six node ring network, under the C-BTMA protocol, with a uniform traffic matrix, $\alpha = 0.01$ and $m = 1$.

nations similar behaviour is observed in general, except for certain quantitative differences. For example, in the simple six node ring, the degree of sensitivity of the network capacity $C(G)$ to the scheduling rate G in the vicinity of G^* differs according to the access scheme. ALOHA and CSMA exhibit the highest sensitivity, while CDMA, CASMA, and the BTMA schemes exhibit the lowest sensitivity. The reason for the greater robustness of BTMA and CASMA is that, given that a node has begun to receive a packet, the reception of this packet may be interfered with only by other transmissions that were initiated during the vulnerable period. The robustness of CDMA is due to the fact that once a reception is initiated, given the assumption of perfect capture it cannot be subsequently interfered with. The ALOHA and CSMA schemes are less robust due to the fact that a packet being received is vulnerable to interference over its entire period of reception. Note that, in ALOHA and CSMA a certain degree of insensitivity to G is still evident since, in the simple six node ring network for example, a factor of 2 or 3 variation in G leads to a variation in $C(G)$ of $\leq 10\%$. Note further that the robustness of BTMA and CASMA is expected to diminish as a increases.

In the sequel, the performance of the various access schemes is studied and compared in 'regular solid' networks and in ring networks, in terms of their capacity and throughput-delay characteristics.

4.2 Nodal Capacity

The optimum network capacity $C(G^*)$ is the most important single parameter that characterizes the performance of a network under a given set of operational protocols. Not only does it give the maximum throughput that a network can support, but in addition it is the most determining factor in the throughput-delay characteristic of a network; indeed, the delay in a network increases from \bar{n} at a throughput approaching zero, to infinity at an asymptote determined by the network capacity. However, since $C(G^*)$ depends

on the type of traffic matrix assumed (either uniform or neighbors-only), in comparing the performance of the various channel access schemes, we focus on the optimum nodal capacity $c(G^*)$. The latter is the same for all traffic matrices that induce balanced link traffic; it is the maximum rate at which a node may transmit successfully over the channel, and hence is a more intrinsic measure of the performance of the access schemes.

For certain networks and access schemes, analyses leading to $c(G^*)$ or $C(G^*)$ have been performed and used to derive numerical results and validate the simulation. These cases consist of (i) the ALOHA schemes in arbitrary multihop topologies, (ii) CSMA, C-BTMA and CASMA in fully connected topologies, and (iii) C-BTMA and CASMA in simple ring topologies for $a = 0$.

(i) **ALOHA schemes in arbitrary multihop topologies.** For the pure ALOHA scheme, we have adapted the approach of [10], where the analysis assumed exponential packet lengths, to the case of fixed packet lengths, while for slotted ALOHA the approach of [19] is used (refer to appendix 1). For the regular topologies considered here with a uniform or neighbors-only traffic matrix, the optimum nodal capacities are expressed as

$$c_{\text{pure ALOHA}}(G^*) = \left(\sqrt{\frac{d}{d+1}} \right)^{d+1} \frac{\sqrt{d+1} - \sqrt{d}}{\sqrt{d}} e^{-(\sqrt{d^2+d}-d)}, \quad (1)$$

$$c_{\text{slotted ALOHA}}(G^*) = \frac{1}{(1+a)(d+1)} \left(\frac{d}{d+1} \right)^d. \quad (2)$$

Note that the nodal capacity for the ALOHA schemes is only dependent on d and is independent of N . Note also that, for the pure ALOHA scheme, the nodal capacity is not a function of the parameter a ; (in fact, of the access schemes under study, it is the only one to exhibit such an independence). Table 1 exhibits the optimum nodal capacity $c(G^*)$ for the various network topologies considered and $a = 0$, as well as the optimum network capacity $C(G^*)$ for uniform traffic.

				Pure ALOHA		Slotted ALOHA	
N	d	Topology	\bar{n}	$c(G^*)$	$C(G^*)$	$c(G^*)$	$C(G^*)$
6	2	Ring	1.80	.078	.260	.148	.494
12	2	Ring	3.27	.078	.286	.148	.543
4	3	Tetrahedron	1.00	.055	.220	.106	.422
8	3	Cube	1.71	.055	.257	.106	.495
20	3	Dodecahedron	2.63	.055	.418	.106	.806
6	4	Octahedron	1.20	.042	.210	.082	.410
12	5	Icosahedron	1.64	.034	.249	.067	.491

Table 1: Network and nodal capacities in regular topologies for uniform traffic requirement for pure and slotted ALOHA protocols, with $a = 0$.

(ii) **CSMA, C-BTMA and CASMA in fully connected topologies.** A simple adaptation of the analysis in [3] to a fully connected network with N identical nodes gives the following approximate expressions for the nodal capacities (refer to appendix 2):

$$c_{CSMA}(G) = \frac{(N-1)Ge^{-a(N-1)G}}{(1+2a)N(N-1)G + Ne^{-a(N-1)G} - 1}, \quad (3)$$

$$c_{C-BTMA}(G) = \frac{(N-1)Ge^{-a(N-1)G}}{(1+3a)N(N-1)G + Ne^{-a(N-1)G} - 1}, \quad (4)$$

$$c_{CASMA}(G) = \frac{(N-1)(N-2)Ge^{-aG(2N-3)}}{(N-1)[N(N-2)(1+4a)G - 2] + Ne^{-aG(N-2)} + N(N-2)e^{-aG(2N-3)}}. \quad (5)$$

The difference between the results for CSMA and C-BTMA is due to the fact that, in the latter case, the period of time during which nodes are blocked is extended by an additional time period a , due to the presence of busy-tone. The difference between the results for CASMA and C-BTMA is due to the fact that, in CASMA, once a transmission

is initiated, the intended receiver is blocked from transmitting after a time units, while the remaining $N - 2$ nodes are blocked after $2a$ time units (when the busy and carrier sense tones are detected). This implies that the period during which a transmission is vulnerable to collisions is increased by a time units over that of CSMA and C-BTMA; furthermore, the period during which nodes are blocked is extended by a time units over that of C-BTMA. Both effects lead to a decrease in the achievable capacity. Note that the difference in performance between all three schemes is rather slight for a small, but becomes more noticable for a large.

(iii) **Simple N -node ring networks with $a = 0$.** When $a = 0$, C-BTMA and CASMA are conflict-free; hence $G^* = \infty$. The capacity is then simply determined by the maximum number of transmissions that can concurrently exist in the network.

C-BTMA: The maximum number of concurrent transmissions in the network is achieved when one in every three nodes is transmitting and the intermediate ones are blocked, and is simply expressed as $\lfloor N/3 \rfloor$. The nodal capacity is obtained by normalizing to the number of nodes and is expressed as*

$$c(\infty) = \frac{1}{N} \left\lfloor \frac{N}{3} \right\rfloor. \quad (6)$$

CASMA: The maximum number of concurrent transmissions in the network is achieved by minimizing the number of *unused* nodes (i.e., neither transmitting nor receiving). Given the CASMA protocol, it is clear that this condition corresponds to the situation whereby a transmitting node is adjacent to its destination and another transmitting node; likewise, a receiving node is adjacent to its sender and another receiving node. Furthermore, the

We note here that, when N is a multiple of 3 and $G^ = \infty$, the maximum number of concurrent transmissions, $N/3$, is achieved by a subset of $N/3$ nodes equally spaced. The nodes in this subset remain the same over time, each achieving a nodal capacity equal to 1, while all others achieve a nodal capacity of 0. We shall nevertheless consider that in this case $c(\infty)$ exists and is equal to $1/3$. For G finite but large, a nodal capacity close to $1/3$ is truly attained by all nodes. However in this case, there may be long periods of time during which the same subset of $N/3$ nodes transmit before another subset of nodes gains access to the channel. Note that in CASMA, a similar effect occurs (for N a multiple of 4), but with respect to subsets of transmissions.

number of unused nodes will vary between 0 and 2 depending on the value of N . The maximum number of concurrent transmissions is expressed as

$$\begin{cases} 1, & N = 2, 3 \\ 2k & N = 4k + l, \quad l = 0, 1, 2; \quad k \geq 1, \\ 2k + 1 & N = 4k + 3 \quad k \geq 1. \end{cases}$$

The nodal capacity is obtained by normalizing to the number of nodes and is expressed as

$$c(\infty) = \frac{1}{N} \begin{cases} 1, & N = 2, 3 \\ 2k & N = 4k + l, \quad l = 0, 1, 2; \quad k \geq 1, \\ 2k + 1 & N = 4k + 3 \quad k \geq 1. \end{cases} \quad (7)$$

Using simulation and analysis whenever possible, we plot in figures 10 to 16 the optimum nodal capacity $c(G^*)$ versus a for the various schemes in the regular solid and 6- and 12-node ring topologies. We note that for all schemes but pure ALOHA (which is independent of a), the nodal capacity decreases as a increases, due to the fact that the information obtained by channel sensing is increasingly out of date; however, for BTMA and CASMA, a greater decrease with a is seen than for the other schemes. In the remaining access schemes, the nodal capacities are less sensitive to a for the following reasons: for slotted ALOHA, equation (2) shows that the capacity varies as $1/(1 + a)$, a quantity which is rather small for $0 \leq a \leq 0.3$ (the range of values depicted in figures 10 to 16). While CSMA is also affected to some extent by a , its performance is primarily limited by collisions due to hidden nodes where these exist, (an effect independent of a). For cases where there are hidden nodes, the nodal capacity of CSMA is low over the entire range of a and thus the effect of a is slight. Only in the case of the fully connected tetrahedron topology (where there are no hidden nodes and the capacity of CSMA is high), is a severe degradation exhibited as the value of a increases (as is also the case for BTMA and CASMA). In CDMA, channel sensed information is not utilized and hence we expect the

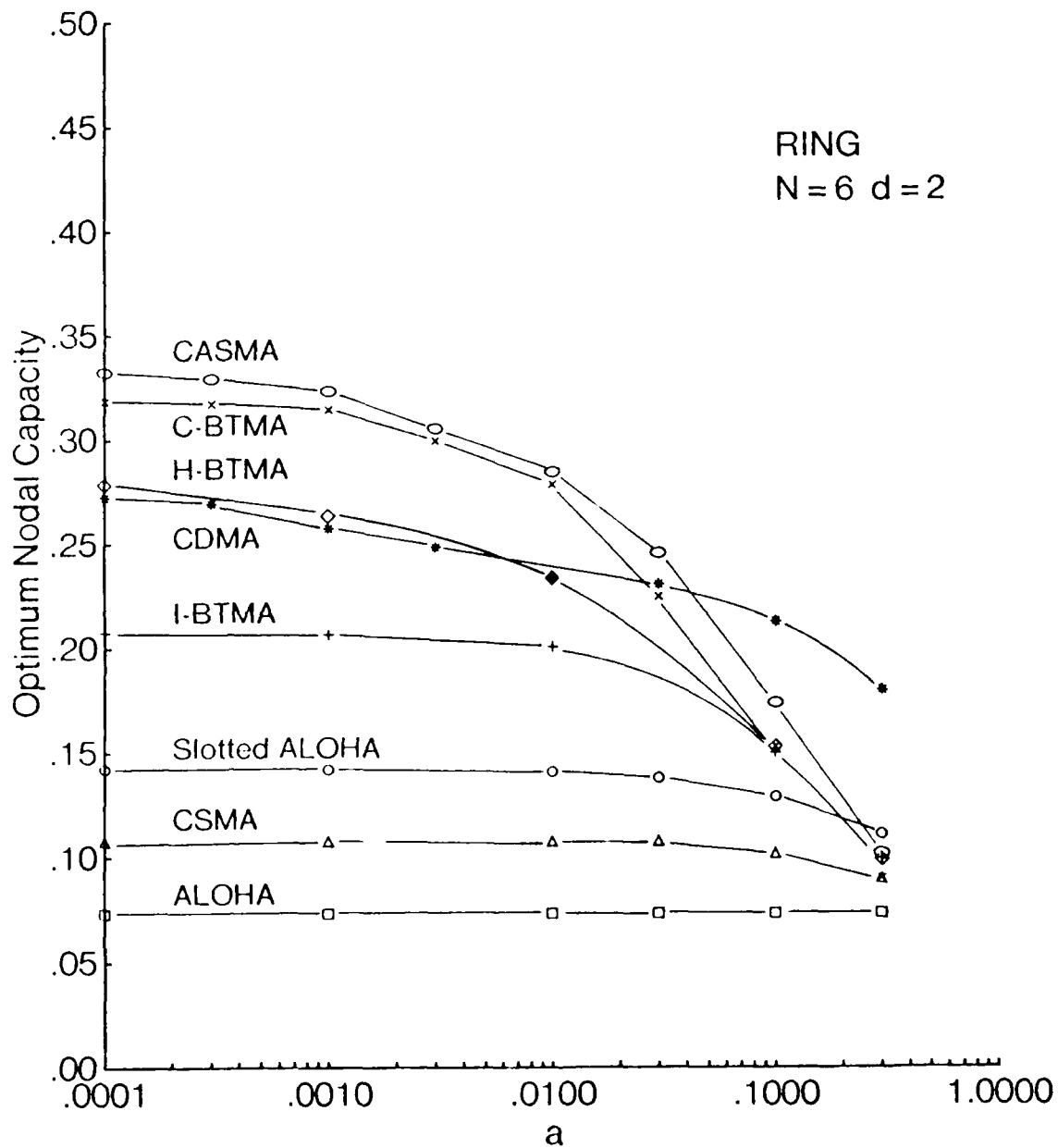


Fig. 10 Optimum nodal capacity versus a for the simple six node ring topology.

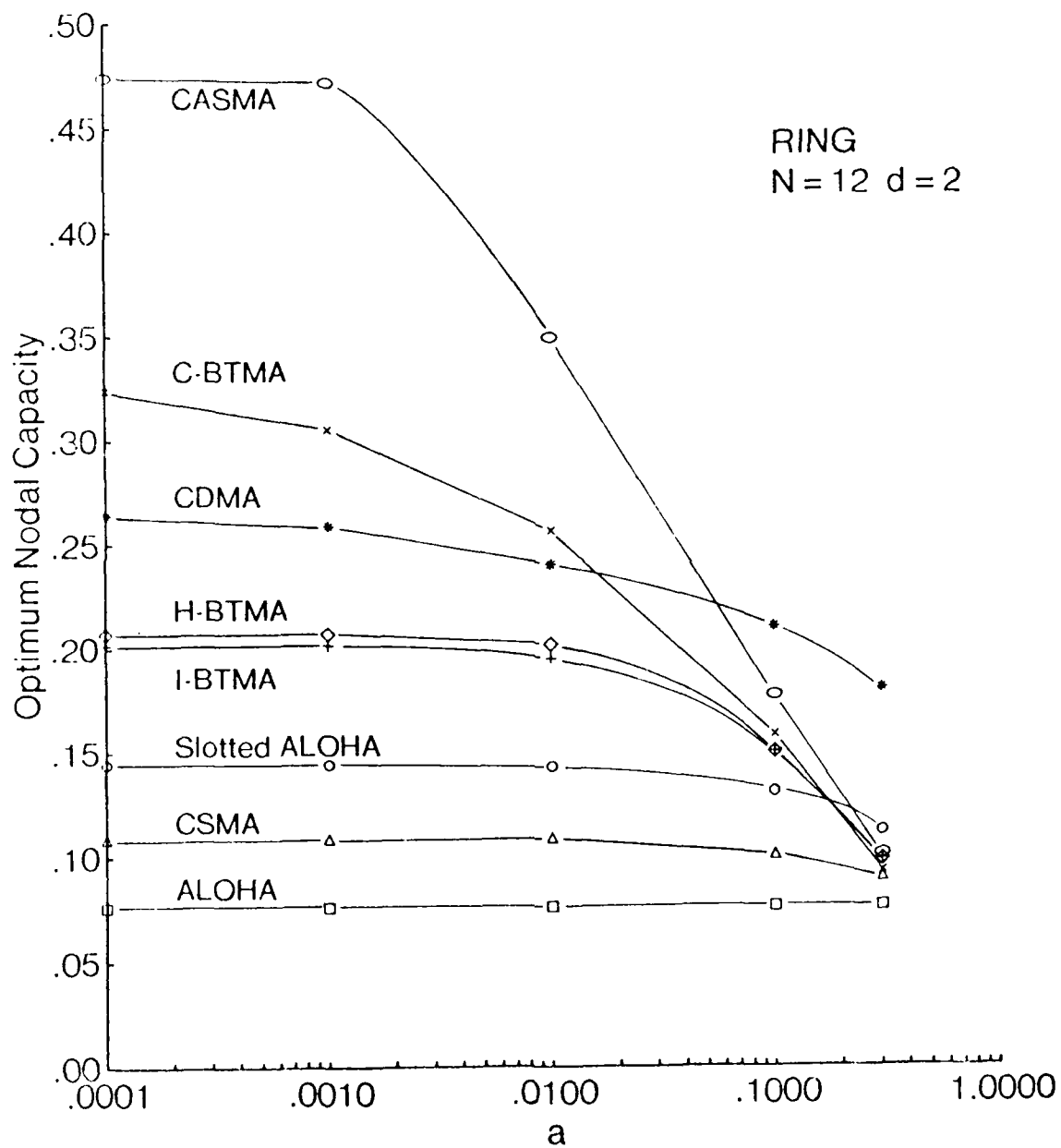


Fig. 11 Optimum nodal capacity versus a for the simple twelve node ring topology.

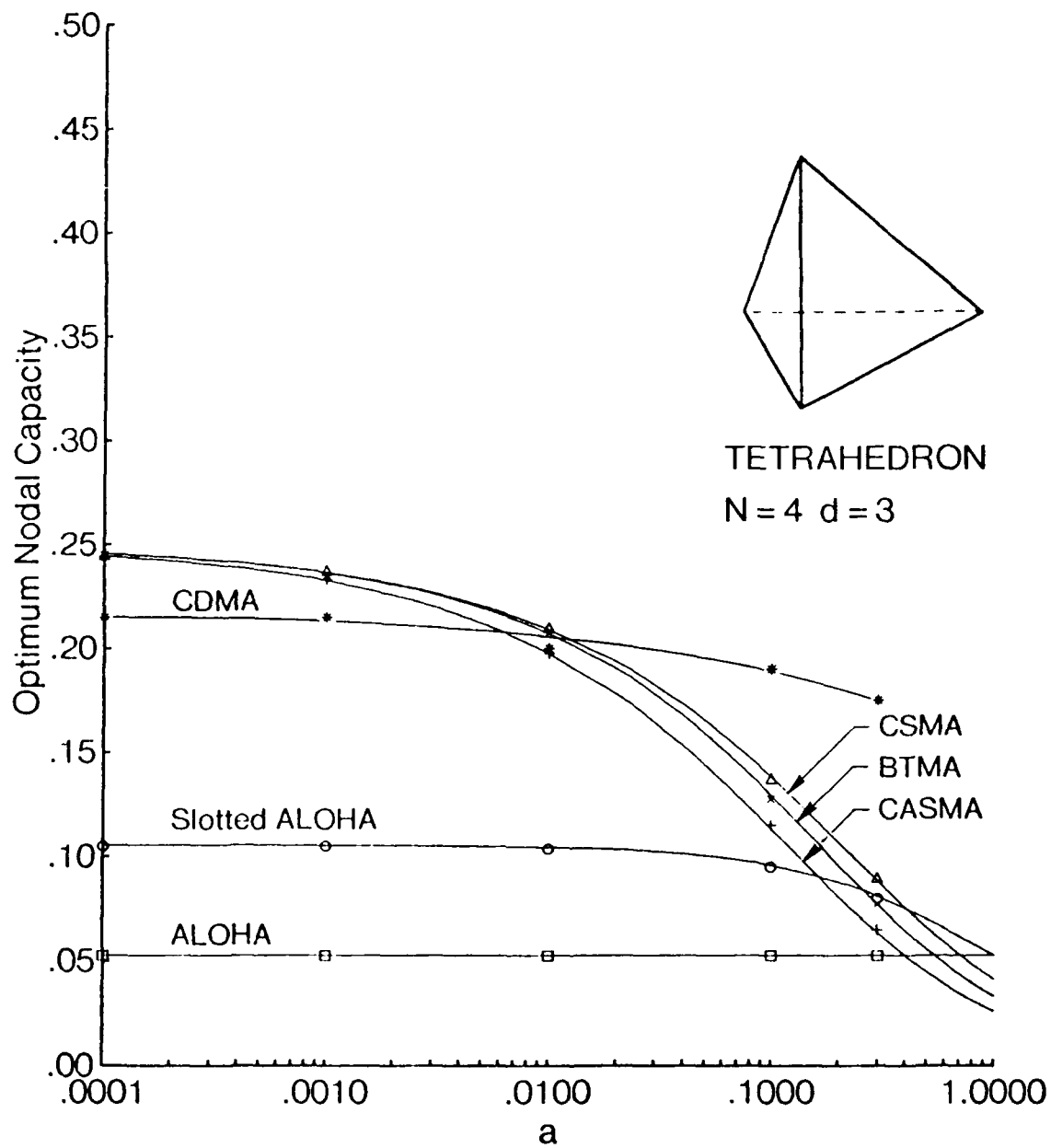


Fig. 12 Optimum nodal capacity versus a for the tetrahedron topology. (All symbols represent simulation results. For CSMA, C-BTMA, CASMA and ALOHA, the curves drawn are obtained from analysis.)

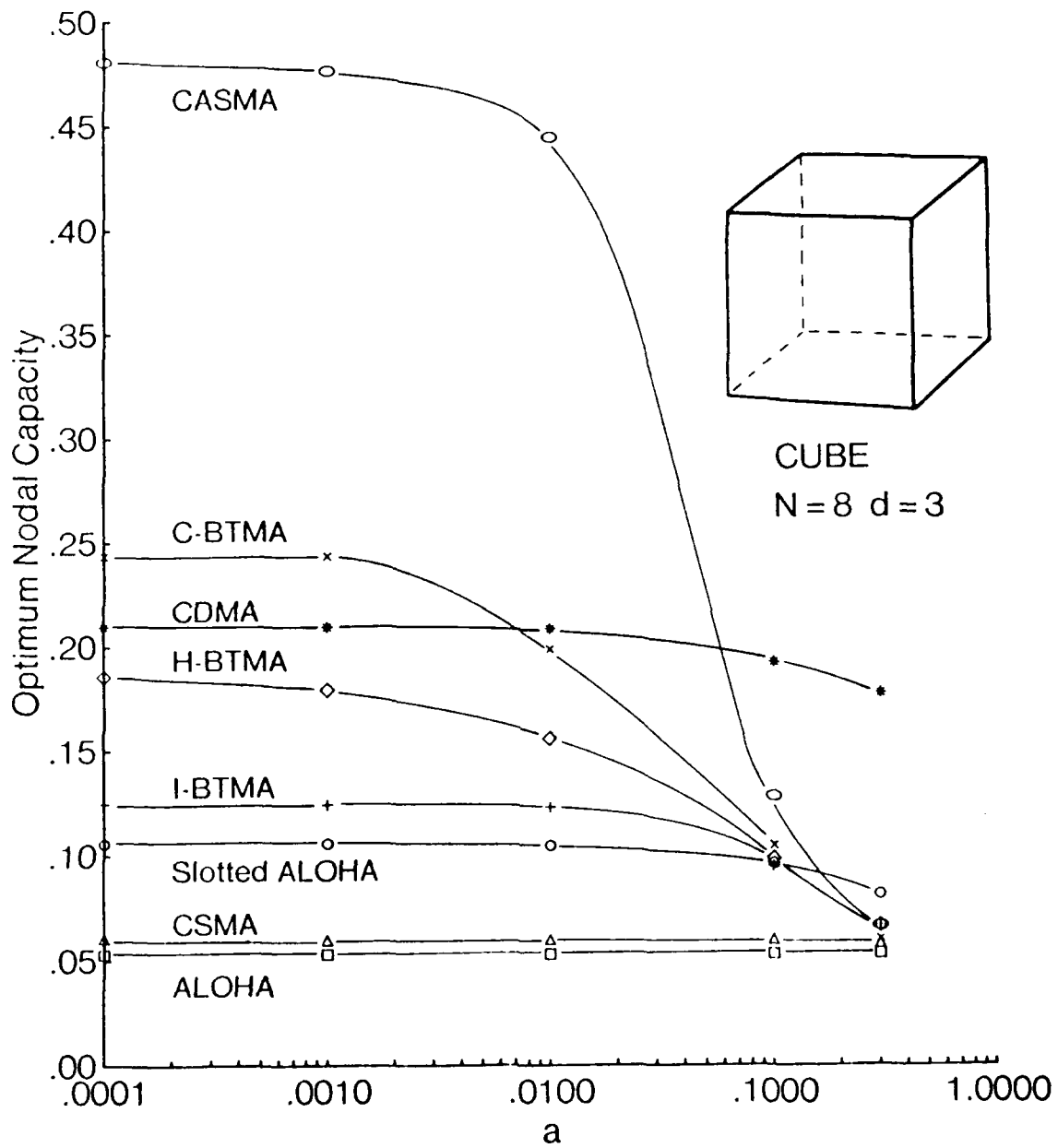


Fig. 13 Optimum nodal capacity versus a for cube topology.

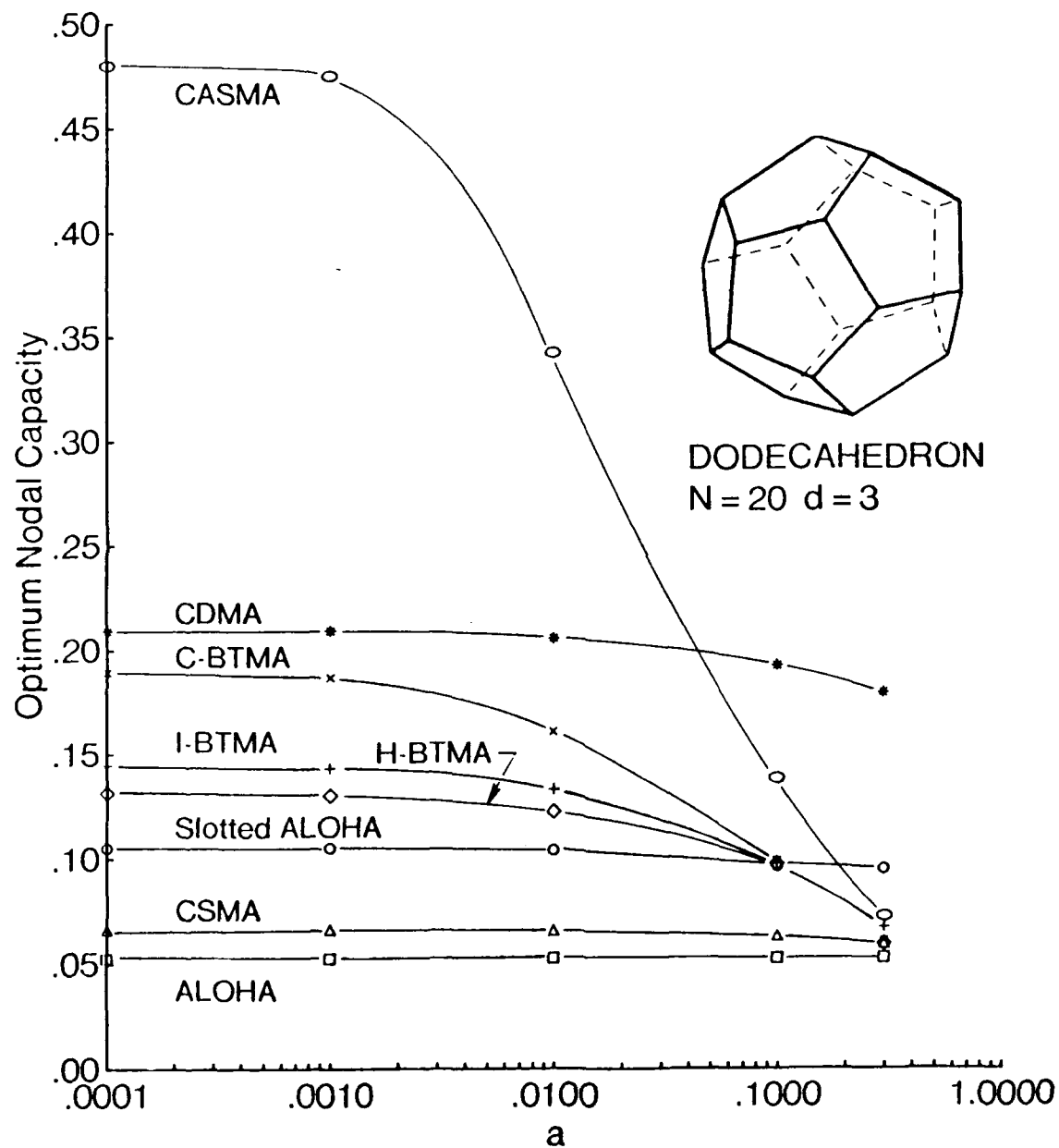


Fig. 14 Optimum nodal capacity versus a for dodecahedron topology.

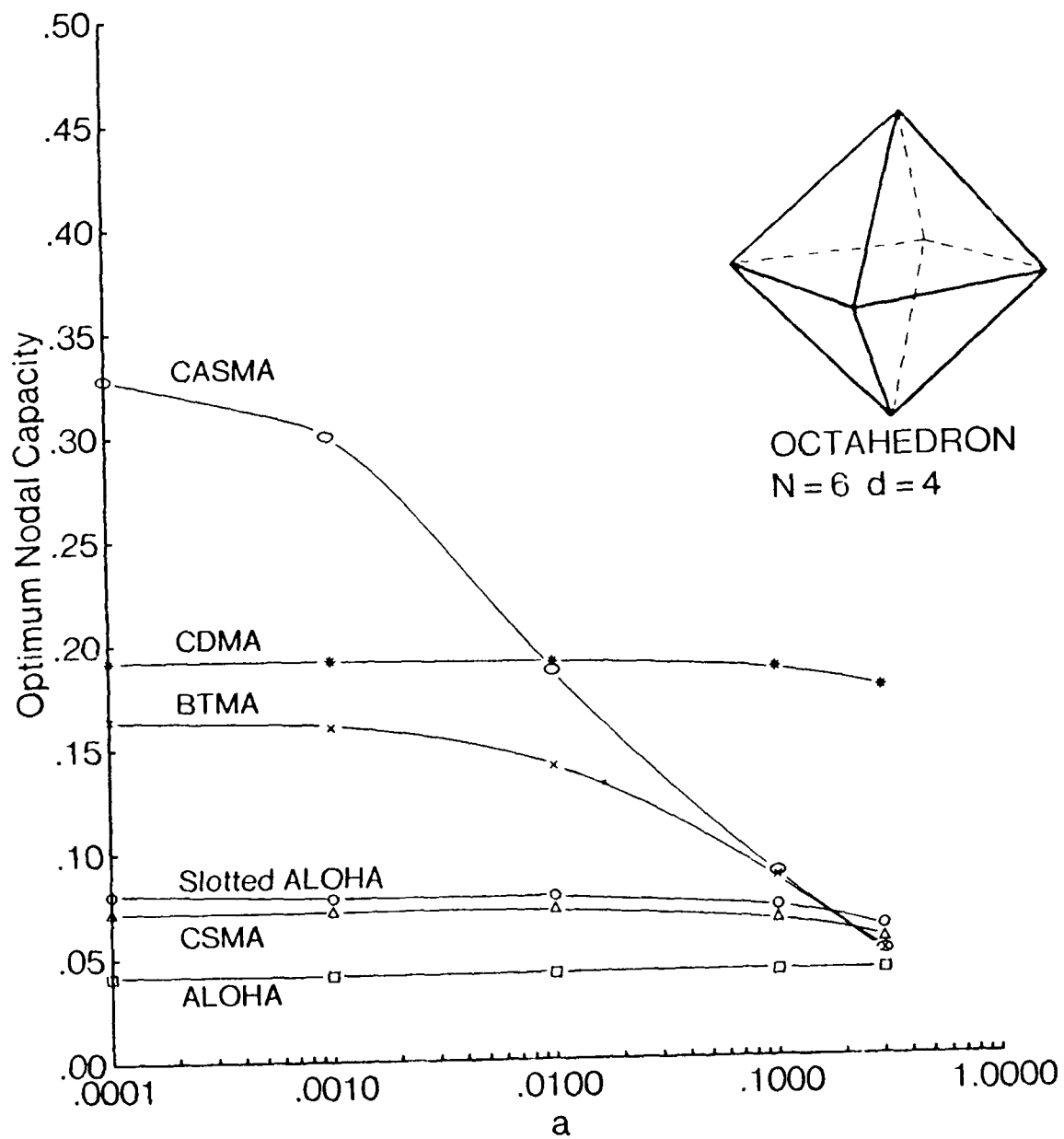


Fig. 15 Optimum nodal capacity versus a for the octahedron topology.

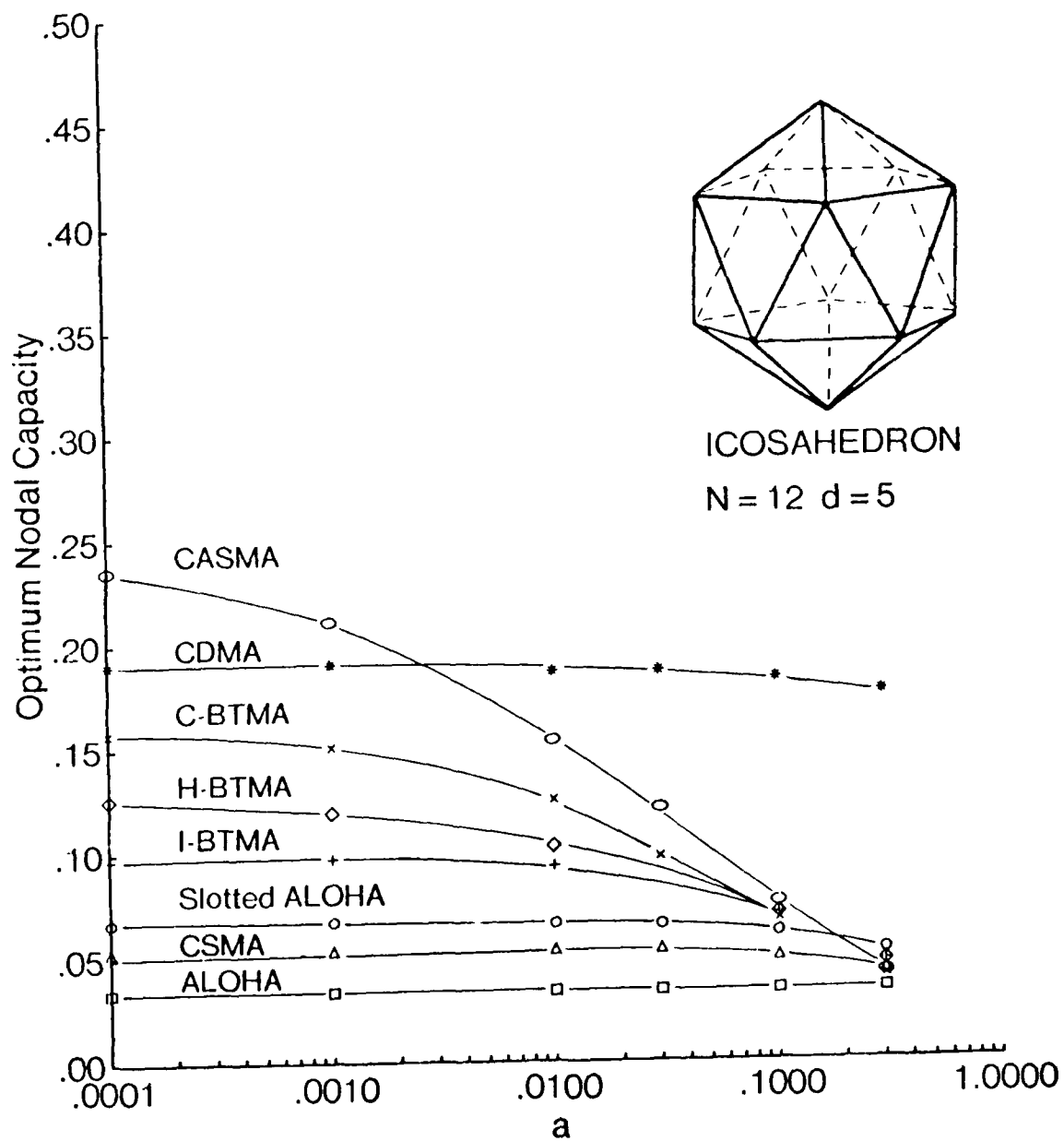


Fig. 16 Optimum nodal capacity versus a for icosahedron topology.

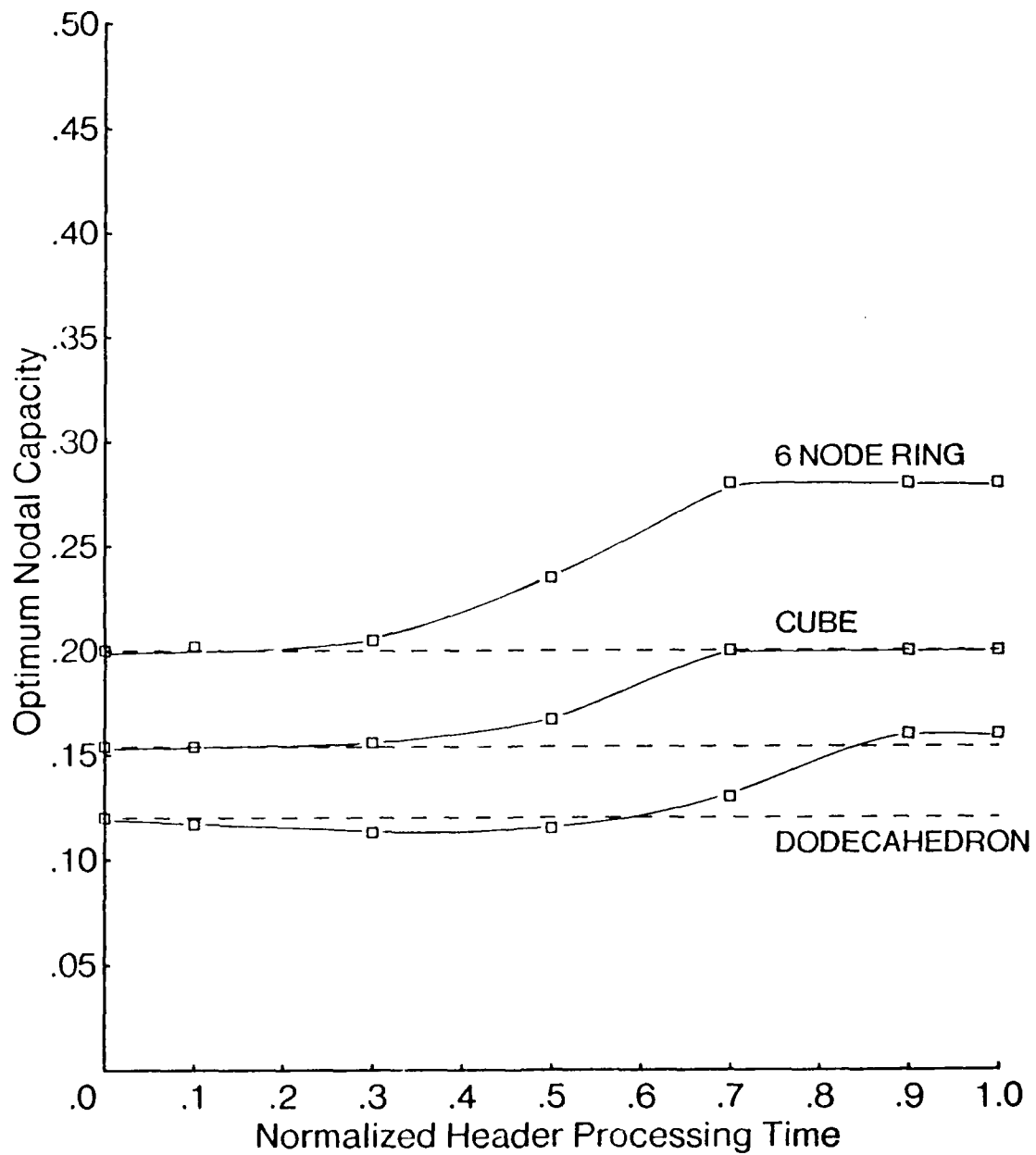


Fig. 17 Optimum nodal capacity versus header processing time for H-BTMA protocol in dodecahedron, cube and six node ring topologies, with $\alpha = 0.01$.

nodal capacity to be basically insensitive to a ; the decrease in the capacity of CDMA with a is due to the fact that, for a large, the probability that a node will begin to transmit while a transmission to it is already on the way, but before the latter transmission is detected, becomes significant. This results in the probability of wasted transmissions increasing with a .

Excluding the CDMA scheme (where the required channel bandwidth may be orders of magnitude greater than for the narrow band schemes), for a small (< 0.1), the protocols may be 'approximately' ranked in order of increasing performance as follows*: pure ALOHA, CSMA, slotted ALOHA, I-BTMA, H-BTMA, C-BTMA and CASMA. One exception to this ordering is CSMA in the (fully connected) tetrahedron topology, where it achieves the highest performance (as expected). The other exception to this ordering occurs in the dodecahedron topology, where the performance of H-BTMA is inferior to both C-BTMA and I-BTMA. Note that for H-BTMA, the capacity achieved depends on the value of header processing time assumed, (here the value is 50% of the packet transmission time in all cases). The effect of the header processing time is clearly seen in figure 17 for the dodecahedron, cube and six node ring topologies. We note that for a header processing time of zero, performance is identical to I-BTMA, while for a header processing time equal to a packet transmission time, performance is identical to C-BTMA. We note further that in the case of the dodecahedron, the capacity of H-BTMA is less than that of both I-BTMA and C-BTMA, over a wide range of header processing times, including the 50% point; for the cube and the ring, the capacity of H-BTMA lies between that of I-BTMA and C-BTMA for all values of header processing time. This rather surprising result in the case of the dodecahedron is somewhat corroborated by the following scenario in H-BTMA: suppose that at a given scheduling point, node i attempts a transmission to node j , where j is currently receiving a packet not destined to it (transmitted by a node

*The cost of the busy tone channel for BTMA, and the activity signalling channel for CASMA is ignored here.

p), has already processed the header of that packet, and hence is not emitting a busy tone. Assume that all other nodes in $N(i)$ are neither transmitting nor receiving. If $\langle i, j \rangle$ is undertaken it will be unsuccessful; furthermore, for a period of time equal to the header processing time h , the nodes in $B = N^*(i) - N(p)$ emit busy tone thereby blocking all nodes in $N(B)$. After h , the nodes in B turn off their busy tone, and for the remainder of the transmission $\langle i, j \rangle$, only the nodes in $N^*(i)$ are blocked (due to carrier sensing). Since $\langle i, j \rangle$ is unsuccessful, the blocking of nodes by $\langle i, j \rangle$ is clearly wasteful, and the more nodes blocked, the greater the waste. Note that in I-BTMA, only the set $N^*(i)$ is blocked for the entire transmission time of $\langle i, j \rangle$, and hence the inefficiency is decreased over the case described above. In C-BTMA, $\langle i, j \rangle$ would have been blocked in the first place, thus entirely avoiding this particular inefficiency. Note that this effect depends on the sizes of the sets $N^*(i)$, B and $N(B)$, and also on the probability that $\langle i, j \rangle$ will be unsuccessful as described above. Thus it is conceivable that in certain cases, the performance of H-BTMA is indeed inferior to both C-BTMA and I-BTMA. Regarding the relative performance of C-BTMA and I-BTMA, the C-BTMA scheme achieves higher throughput than the I-BTMA scheme in all networks under study, indicating that the potential collisions permitted by the I-BTMA scheme are more harmful to performance than the blocking of potentially successful transmissions caused by C-BTMA. Note that for $a > 0.1$, the capacity of BTMA and CASMA continues to decrease, becoming less than that of slotted ALOHA, and approaching that of CSMA and pure ALOHA.

We now examine in more detail the performance of certain access schemes in simple ring networks with different values of N . We limit the discussion to the case $a = 0$ for which we make use of equations (6) and (7). In figure 18, we plot the nodal capacity $c(G^*)$ versus N for the ALOHA, Slotted ALOHA, C-BTMA and CASMA schemes. Figure 18 suggests that, in the 6-node ring for a small, CASMA and C-BTMA achieve similar performance, while in the 12-node ring CASMA achieves a higher performance than C-BTMA, which explains why this is indeed observed in figures 10 and 11. Note that as $N \rightarrow \infty$, the nodal

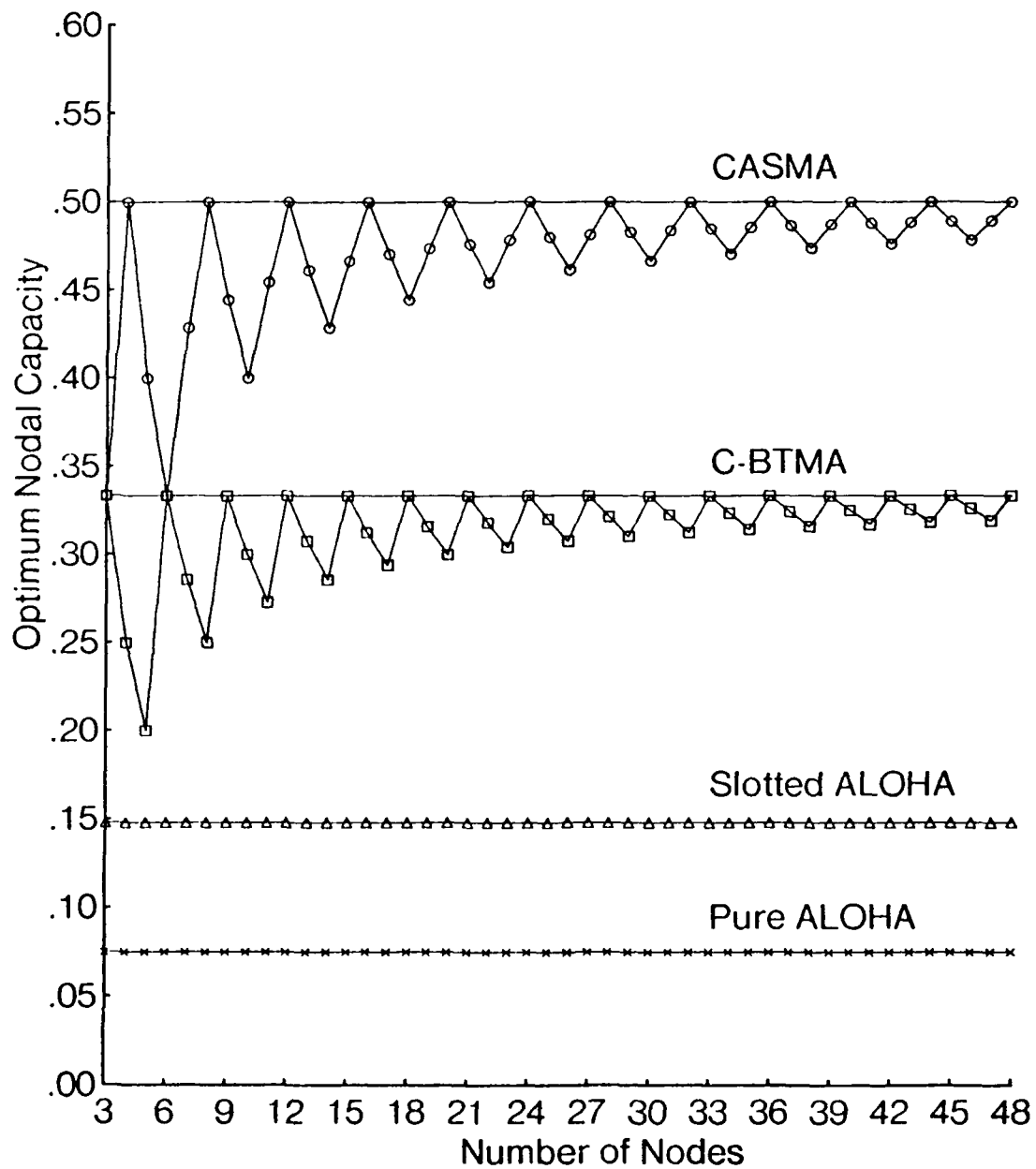


Fig. 18 Optimum nodal capacity versus number of nodes for the simple ring topology.

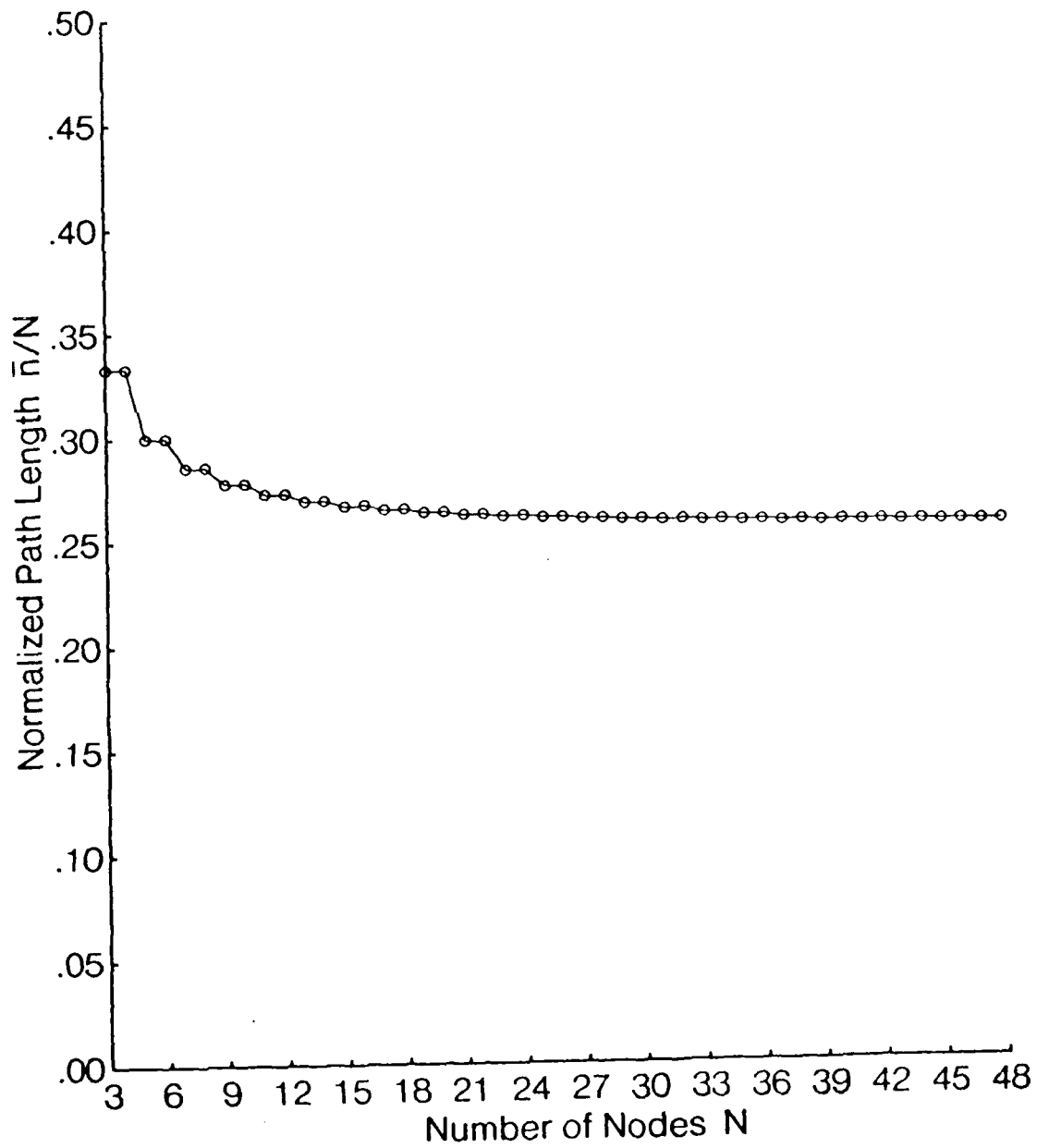


Fig. 19 Normalized path length versus number of nodes for the simple ring topology.

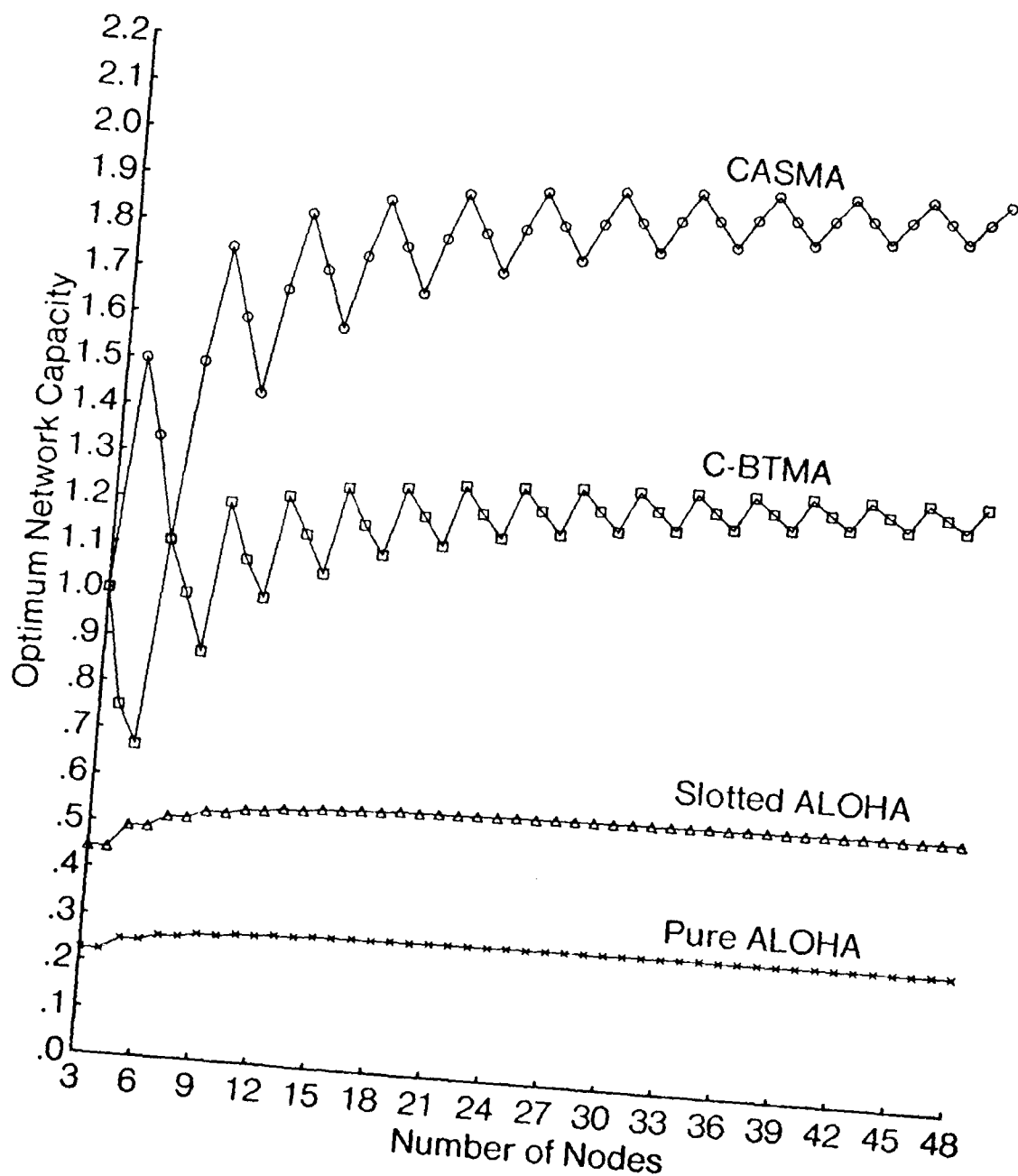


Fig. 20 Optimum network capacity versus number of nodes for the simple ring topology.

capacity for each access scheme becomes insensitive to N and approaches a limit. For the case of the uniform traffic matrix, from [19],

$$\bar{n} = \lfloor (N+1)/2 \rfloor \left(1 - \frac{\lfloor (N-1)/2 \rfloor}{N-1}\right). \quad (8)$$

The graph of \bar{n}/N versus N is shown in figure 19. Note that $\lim_{N \rightarrow \infty} \bar{n} = N/4$. In figure 20, we plot the network capacity $C(G^*)$ versus N for the uniform traffic matrix. Since in the case of the ring, \bar{n} is proportional to N , it is not surprising to see that $C(G^*)$ approaches a limit as $N \rightarrow \infty$ as well. The results of figures 18 and 20 can be compared with those in [10] where the nodal capacity of C-BTMA and ALOHA (among others) was analyzed for the case of exponential packet lengths. We find that there is a minor difference (6%) for the case of ALOHA, while the results are identical for C-BTMA. We attribute the former difference to the different assumptions concerning packet length distribution, since, in pure ALOHA, once a transmission is undertaken, the probability of success is dependent on the packet length; in C-BTMA for $a = 0$, once a transmission is undertaken, the probability of success is unity, and is thus independent of the packet length.

4.3 Effect of d on the Nodal Capacity

In figures 21 and 22, we plot for $a = 0.01$ and 0.1 respectively the nodal capacity versus d for various access schemes in the regular solids and simple rings. The results clearly indicate that the nodal capacity $c(G^*)$ decreases as the nodal degree d increases. Note that there is a variation in $c(G^*)$ with N for d and a fixed, due to the finite values of N in the regular solids and simple rings considered. However, this variation is less pronounced when a is large. Furthermore, as remarked earlier for simple rings, the variation is also less pronounced for large N . Thus we conclude that d is the topological parameter which affects performance the most. Note however that the CDMA scheme is seen to be less affected by d than are the narrow band schemes, with the difference in performance between CDMA

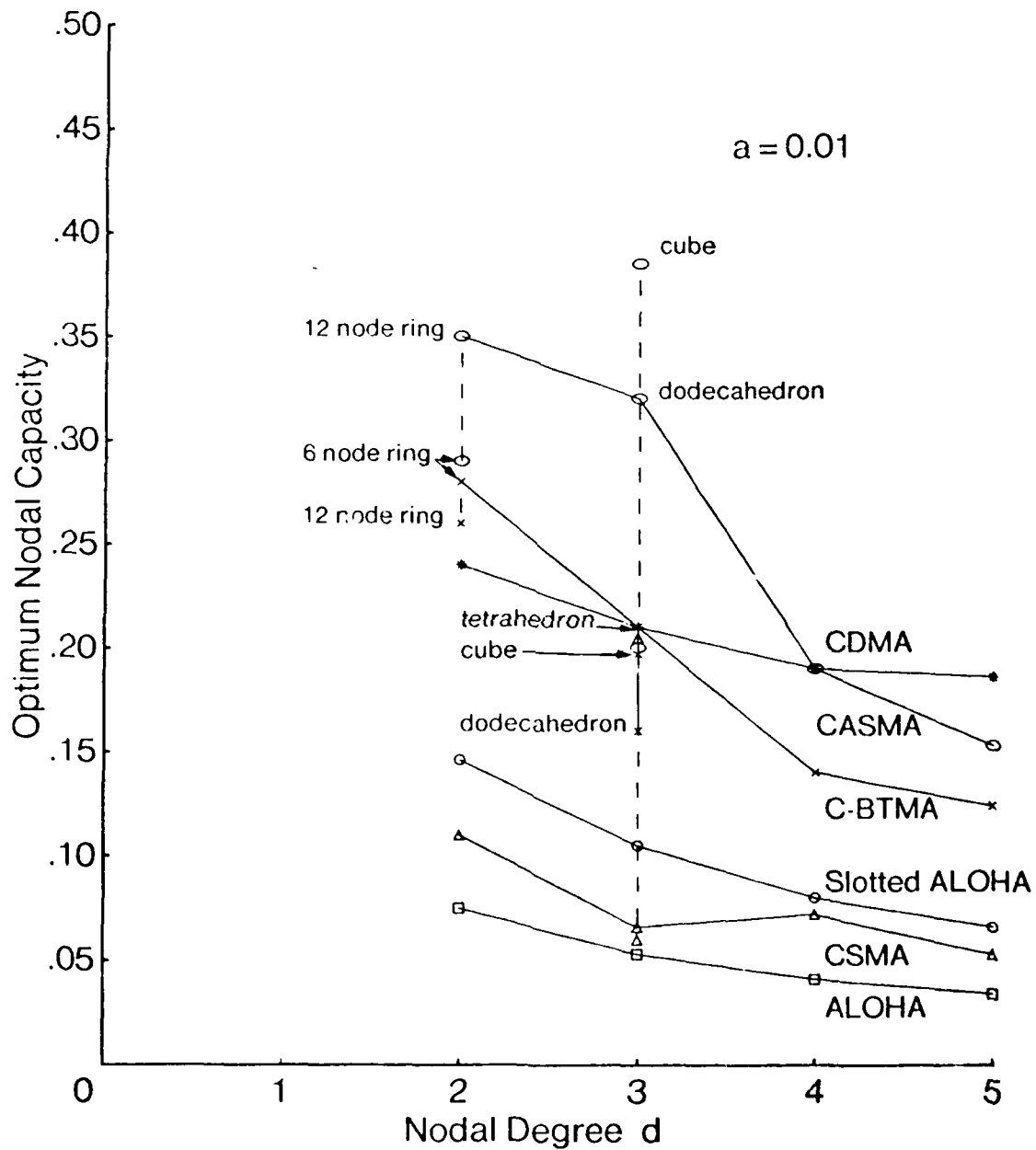


Fig. 21 Optimum nodal capacity versus degree for regular solid and simple ring networks, with $a = 0.01$.

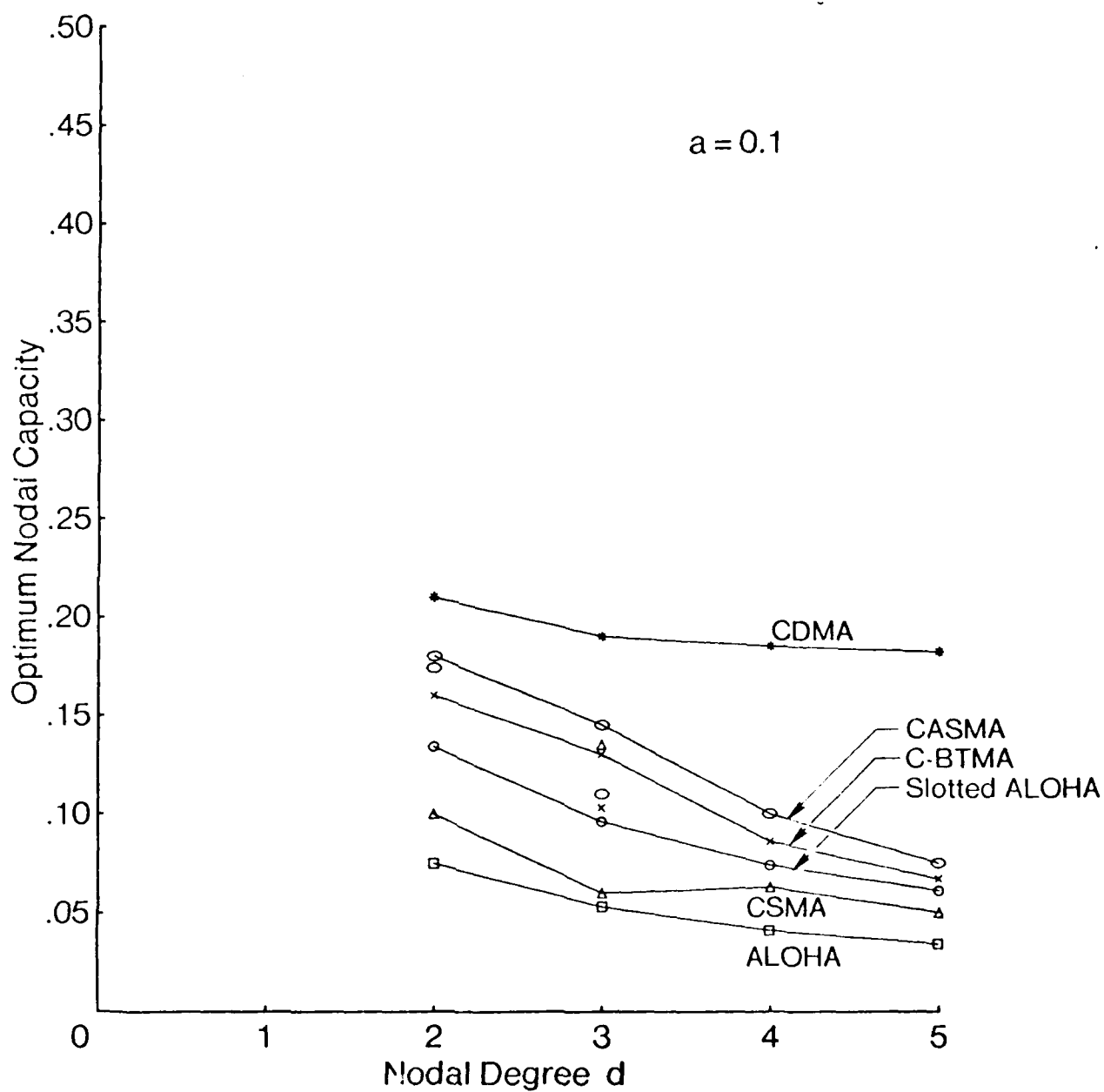


Fig. 22 Optimum nodal capacity versus degree for regular solid and simple ring networks, with $a = 0.1$.

and the other schemes increasing with d . This is due to the directional capture assumption of CDMA as described in section 3, which enables it to achieve a potentially higher number of successful, concurrent transmissions than the narrow band protocols.

In order to further study the effect of the degree d on nodal capacity without constraints on N and d , we consider multiconnected ring networks with a neighbors-only traffic matrix. Note that, in this case, contrary to the simple ring ($d = 2$) and the regular solid networks considered previously, the link traffic processes under the CSMA, BTMA and CASMA access schemes are no longer statistically identical. This is due to the fact that for the aforementioned access schemes, the probability of successful reception p_s is different on each link; (p_s is not link dependent for ALOHA and CDMA, hence all link traffic processes are statistically identical for these schemes). For example, consider a multiconnected ring with N nodes of degree 4, operating under CSMA with $a = 0$. Consider the nodes to be numbered sequentially and consider transmissions from node 1 to its neighbors (i.e, nodes 2, 3, $N - 1$, and N). The transmission $\langle 1, 2 \rangle$ is vulnerable to transmissions from node 4 only, (the other neighbors of 2 being blocked by carrier sensing), while $\langle 1, 3 \rangle$ is vulnerable to transmissions from both nodes 4 and 5. Let $S'(\gamma, m, G) \triangleq 2NS_{12}(\gamma, m, G)$ and $S''(\gamma, m, G) \triangleq 2NS_{13}(\gamma, m, G)$; these represent the sum of link throughputs summed over all links which are statistically identical to $S_{12}(\gamma, m, G)$ and $S_{13}(\gamma, m, G)$ respectively. We expect that $S_{12}(\gamma, m, G) \geq S_{13}(\gamma, m, G)$ and hence $S'(\gamma, m, G) \geq S''(\gamma, m, G)$ for all γ . This expectation is confirmed in figure 23 where $S'(\gamma, m, G)$, $S''(\gamma, m, G)$ and their sum $S(\gamma, m, G)$ (the network throughput) are plotted versus the offered input traffic rate γ , for the case of $N = 12$, $d = 4$, $a = 0.01$, $m = 50$ and $G = 0.5$. Furthermore, we note that $S'(\gamma, m, G) = S''(\gamma, m, G)$ for $\gamma < \gamma_1$, $S'(\gamma, m, G) > S''(\gamma, m, G)$ for all $\gamma > \gamma_1$, and $S'(\gamma, m, G)$ and $S''(\gamma, m, G)$ approach limits $C'(G)$ and $C''(G)$ respectively for γ large, as indicated in figure 23. (Note that the ratio $C'(G)/C''(G)$ can be altered by varying the queue scheduling distribution; however, in this work, we consider only a uniform queue scheduling distribution). The additional complexity in the behaviour of

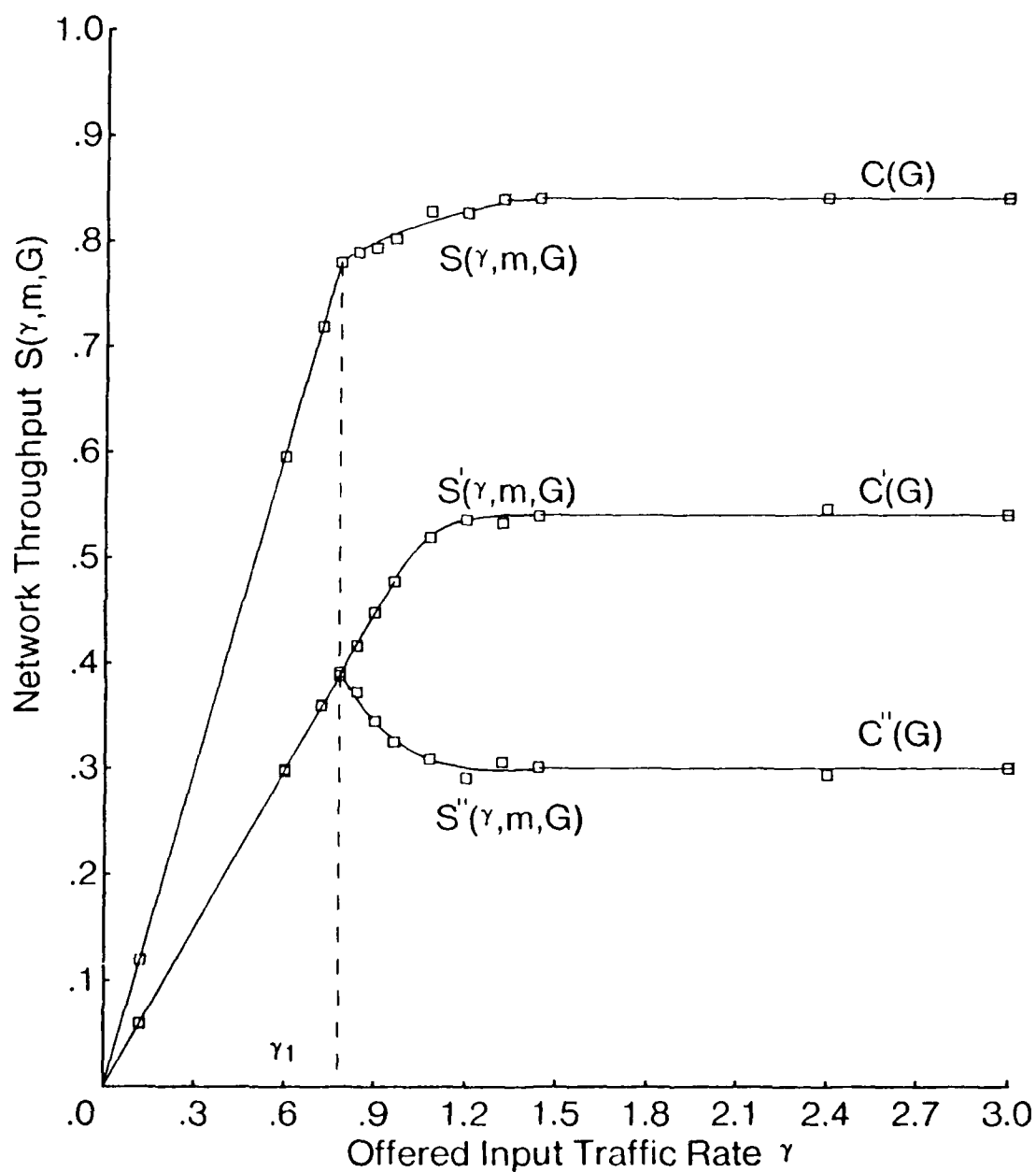


Fig. 23 Network throughput $S(\gamma, m, G)$ versus offered input traffic rate γ , in a 12-node multiconnected ring of degree 4, under the CSMA protocol with a neighbors-only traffic matrix, $a = 0.01$, $m = 50$ and $G = 0.5$.

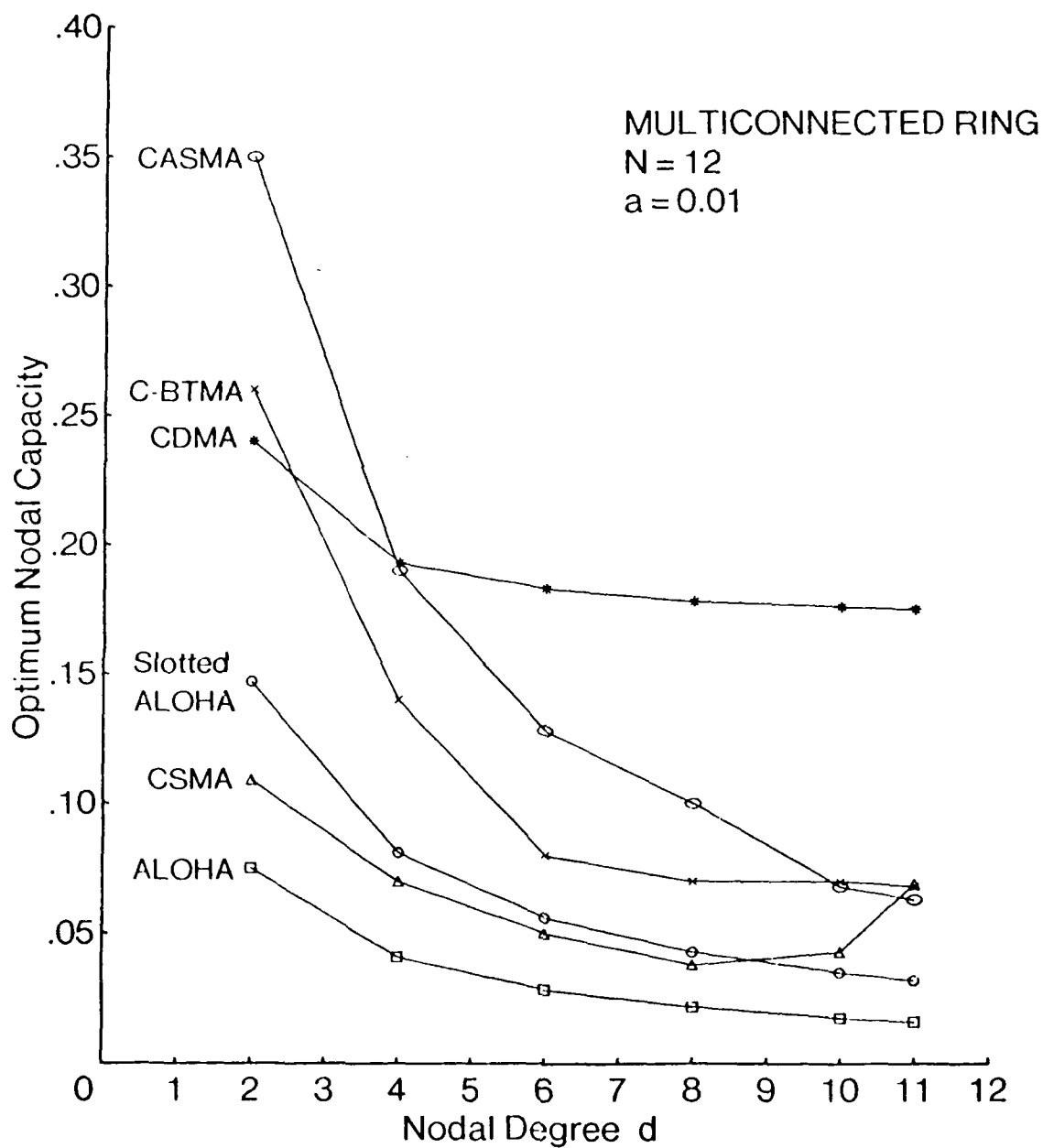


Fig. 24 Optimum nodal capacity versus degree for 12-node multiconnected ring, with $\alpha = 0.01$.

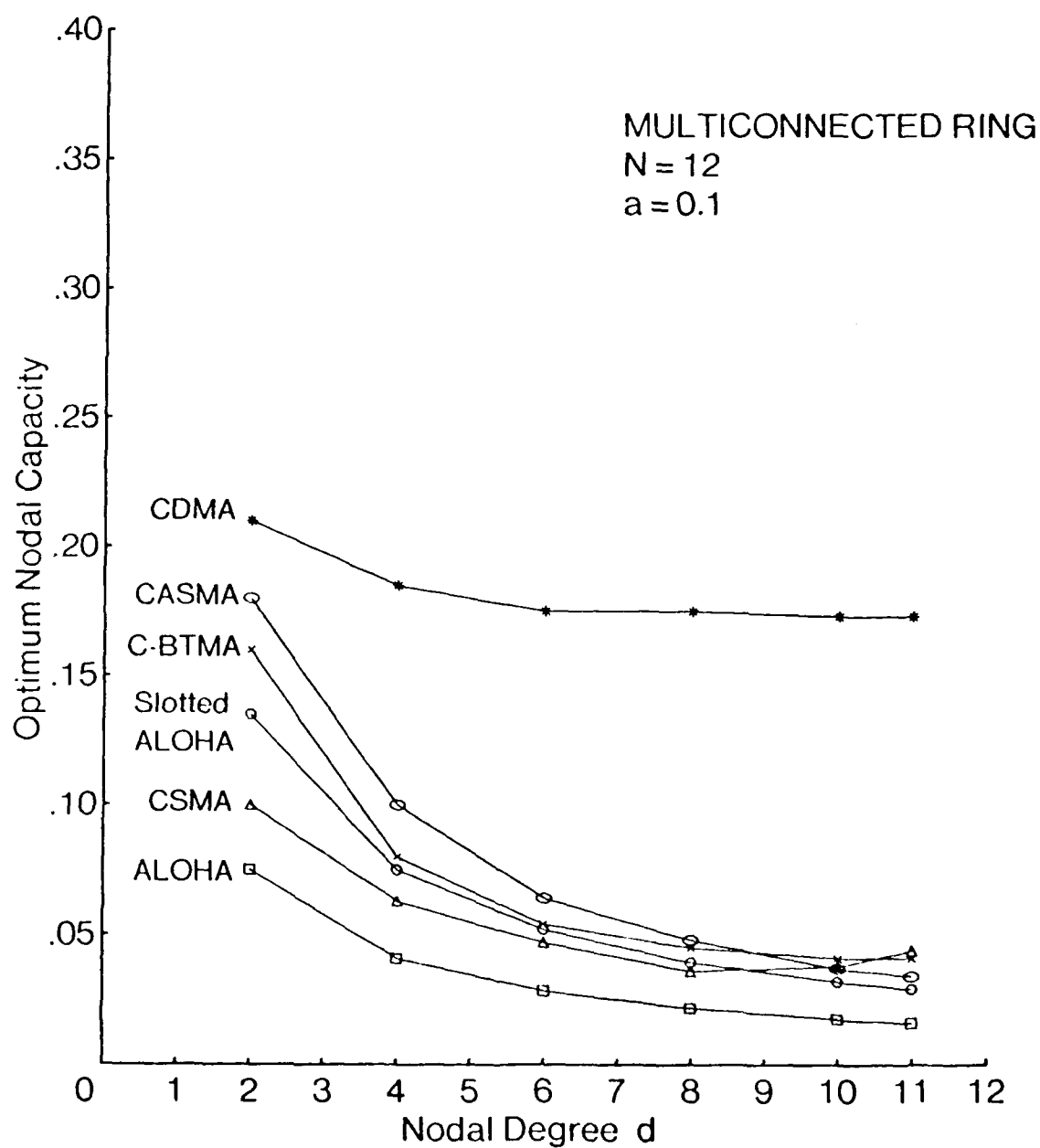


Fig. 25 Optimum nodal capacity versus degree for 12-node multiconnected ring, with $a = 0.1$.

such a network indicates the reason why, in this report, we have chosen to focus only on entirely regular topologies. In a forthcoming report, the more complex non-regular networks will be studied.

In figures 24 and 25, for $a = 0.01$ and $a = 0.1$, the optimum nodal capacity for various access schemes considered are plotted versus the nodal degree d for $N = 12$. The results generally confirm those of figures 21 and 22, and allow us to observe the effect of d for $d > 5$; in particular, we note that for large d , the capacity of CDMA is significantly higher than of the narrow band schemes. We also observe that, in multiconnected rings, the performance of CSMA first decreases with d and then increases as the connectivity of the network increases; at $d = N - 1$, as expected, the performance of CSMA is the best among the narrow band schemes.

4.4 Throughput - Delay Performance

For the case of uniform traffic and finite values of input traffic rate γ , we examine the throughput-delay tradeoff for the various access schemes in two representative topologies, namely, the simple six node ring and the icosahedron. Unlimited acceptance of both new and transit packets (i.e., $m = \infty$) and a value of $a = 0.01$ are assumed. For $\gamma \leq C(G^*)$, we find that the network delay $D(\gamma, \infty, G)$ is minimized by a particular value of G denoted by $G_{opt}(\gamma)$, for each γ . This is depicted in figure 26 for the case of CSMA in the simple six node ring topology. Note that as $\gamma \rightarrow 0$, $G_{opt}(\gamma) \rightarrow \infty$, and as $\gamma \rightarrow C(G^*)$, $G_{opt}(\gamma) \rightarrow G^*$; refer to figure 8 and the discussion pertaining thereto. Furthermore, we observe that the sensitivity of $D(\gamma, \infty, G)$ to G increases with γ ; such behaviour had been encountered previously in the context of single-hop, fully connected networks [3], [20]. In figures 27 and 28, we plot the minimum network delay $D(\gamma, \infty, G_{opt}(\gamma))$ versus the network throughput $S(\gamma, \infty, G_{opt}(\gamma))$ in the simple six node ring and the icosahedron topologies for all access schemes under consideration. Note that all curves share certain properties,

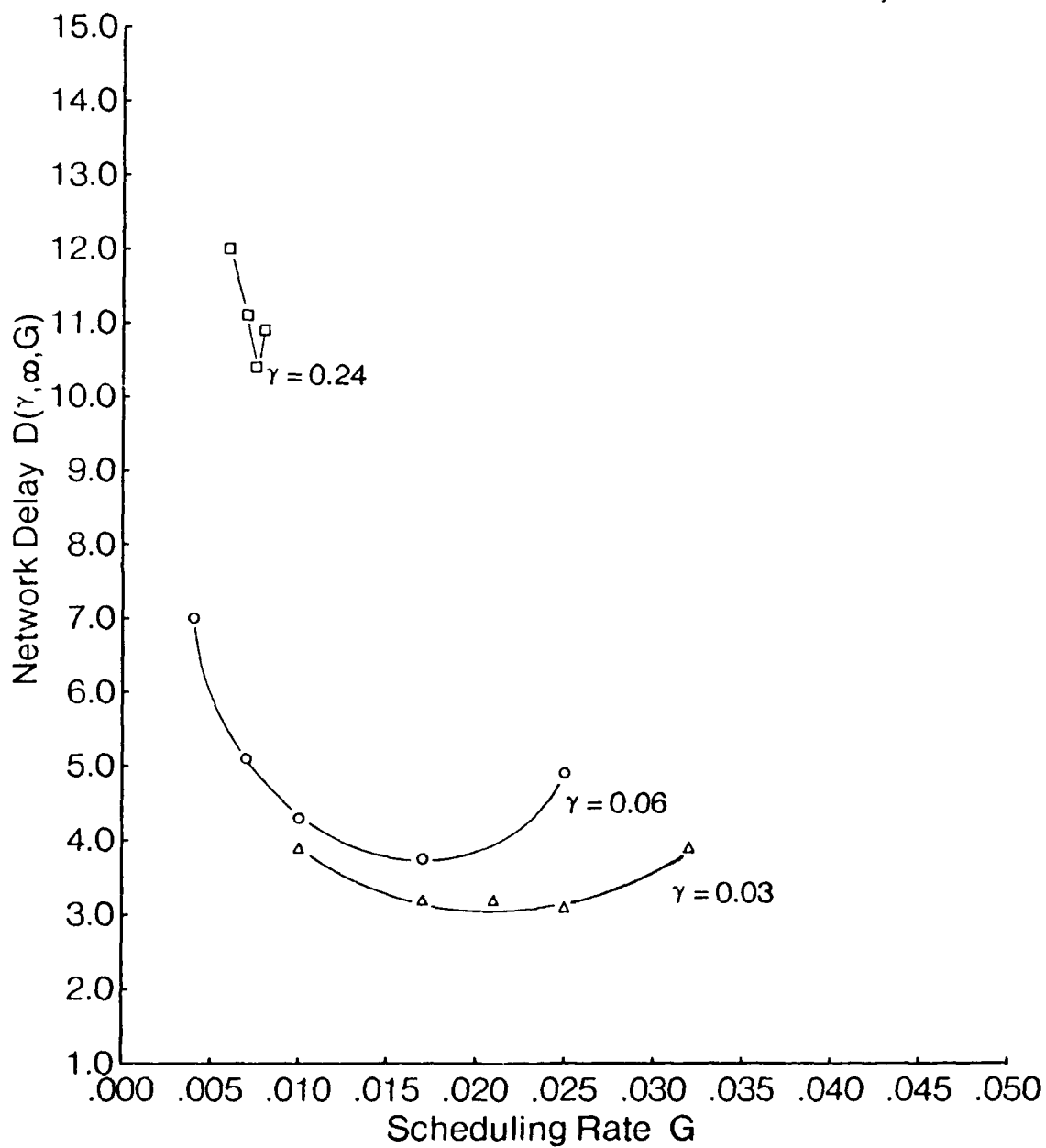


Fig. 26 Network delay versus scheduling rate for CSMA protocol in the simple six node ring topology, with uniform traffic and $\alpha = 0.01$.

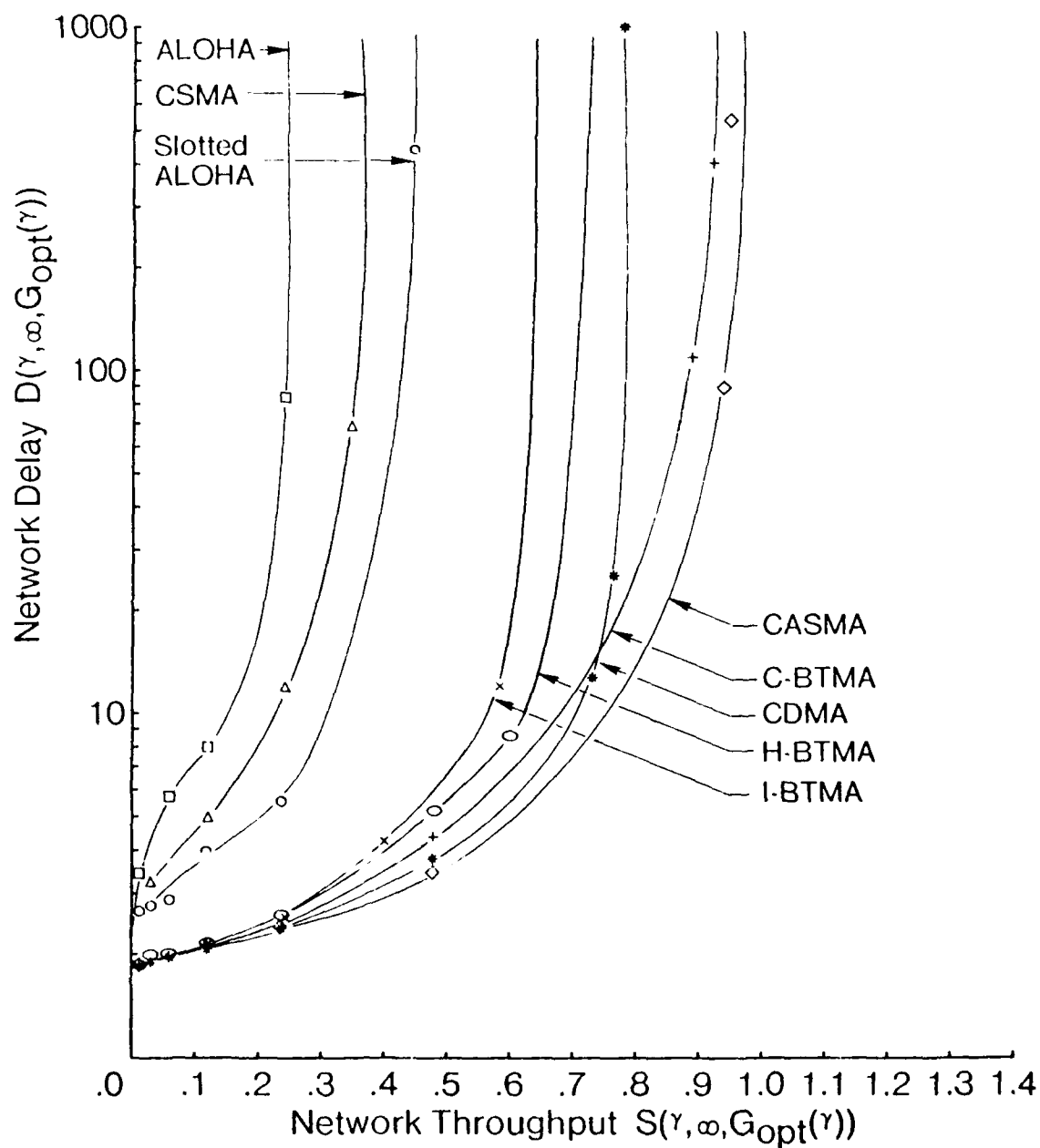


Fig. 27 Network delay versus network throughput for the simple six node ring topology, with uniform traffic and $\alpha = 0.01$.

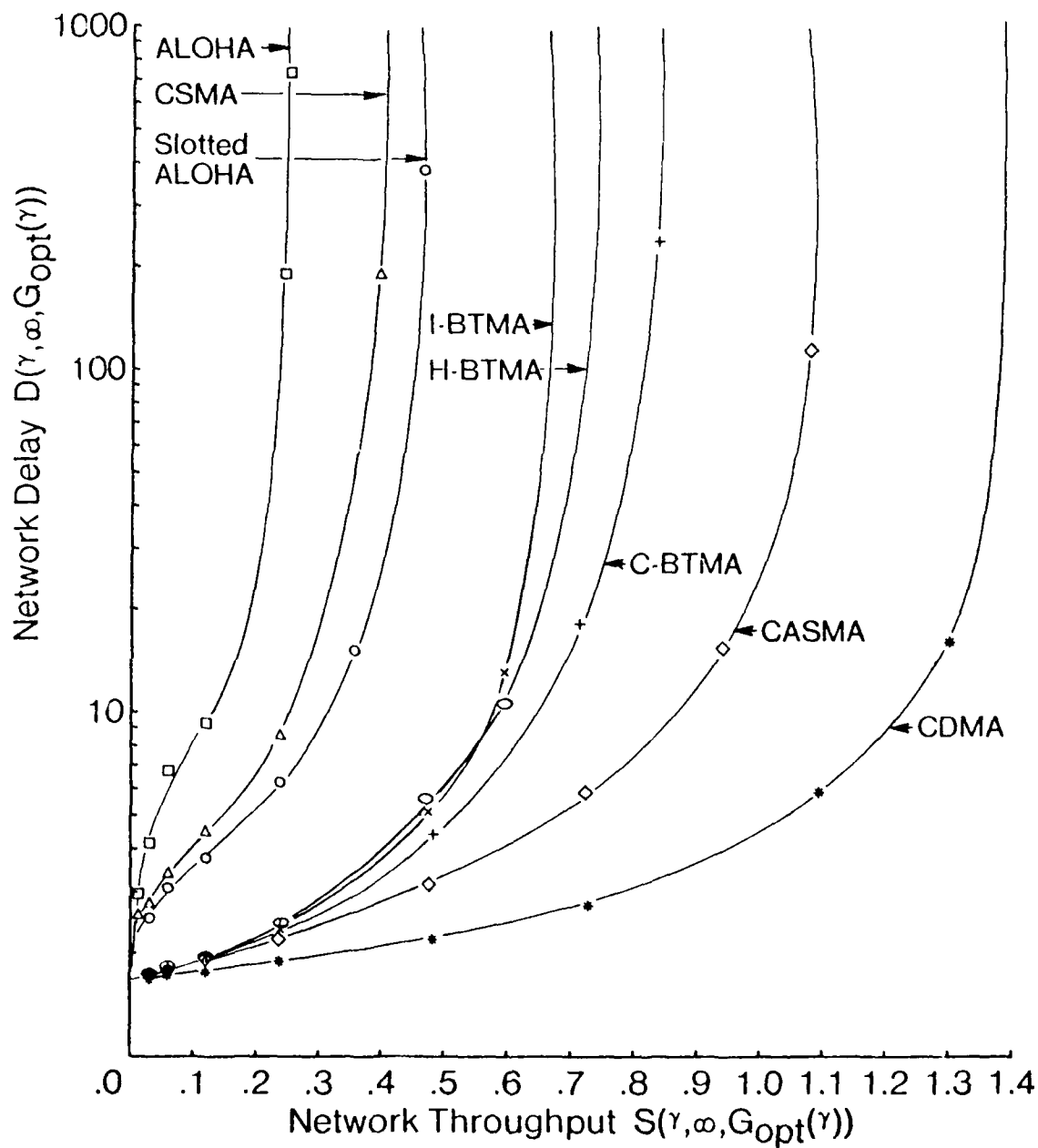


Fig. 28 Network delay versus network throughput for the icosahedron topology, with uniform traffic and $a = 0.01$.

namely, $\lim_{\gamma \rightarrow 0} D(\gamma, \infty, G_{opt}(\gamma)) = \bar{n}$, (the average path length), $\lim_{\gamma \rightarrow C(G^*)} S(\gamma, \infty, G_{opt}(\gamma)) = C(G^*)$, and $\lim_{\gamma \rightarrow C(G^*)} D(\gamma, \infty, G_{opt}(\gamma)) = \infty$. Note further that the ordering of the access schemes in terms of the maximum network throughput is as predicted in figures 10 and 16 for $a = 0.01$.

5. Concluding Remarks

In this report, we have studied the performance of multihop packet radio networks with regular structure. The effect of the nodal scheduling rate, and the input flow control on performance was detailed, and the sensitivity of the performance measures to these variables was explored. It was found that network delay was much more sensitive to the nodal scheduling rate than was network throughput. Regarding flow control, it was seen that when the flow control scheme caused blocking at the network input, a reduction in throughput resulted. The performance of the various access schemes was compared in terms of their nodal capacity, and throughput-delay characteristics. The performance of CSMA was shown to degrade severely in multihop networks. Regarding the effect of a , the performance of the BTMA and CASMA schemes were seen to be rather sensitive to this parameter, but for a small, relatively high capacities were achieved by these schemes as compared with CSMA and ALOHA (by factors of typically ≥ 3). The CDMA scheme also achieved relatively high throughput and was also only slightly sensitive to a . Regarding the effect of nodal degree, it was seen that nodal capacity decreased with d ; however, a smaller decrease was observed for CDMA than for the narrow band schemes. It was also noted that for certain networks of the same nodal degree but with a different number of nodes, different nodal capacities resulted. It is believed that this effect is due to the finite size of the networks considered. Finally, it should be kept in mind in comparing the performance of these schemes that a penalty has not been assessed neither for the busy

tone in BTMA, nor for the activity signalling in CASMA, nor for the additional bandwidth required for spread spectrum operation in CDMA. However, with reference to BTMA, in environments where the channel bandwidth is the limiting resource, the improvement in channel utilization achieved may well more than compensate for the cost of the busy tone.

Appendix 1: Nodal Capacity of pure and slotted ALOHA in Arbitrary Topologies

Let G_{ij} be the rate of the scheduling process at node i for packets destined to node j . It is assumed that G_{ij} is non-zero only if $j \in N^*(i)$, ($i = 1, \dots, N$). Let $G_i = \sum_{j \in N^*(i)} G_{ij}$. Let c_{ij} denote the average number of packets transmitted successfully from node i to node j per packet transmission time, and let $c_i = \sum_{j \in N^*(i)} c_{ij}$.

For each node i , c_{ij} is zero for $j \notin N^*(i)$, while for $j \in N^*(i)$

$$\frac{c_{ij}}{G_{ij}} = \Pr\{\text{scheduling point at node } i \text{ results in a transmission}$$

and the transmission is successful}

$$= \Pr\{\text{node } i \text{ is not transmitting}\} \Pr\{\text{transmission } \langle i, j \rangle \text{ is successful}\},$$

$$= P_i^I P_{ij}^s$$

Pure ALOHA: From renewal theory arguments, $P_i^I = 1/(1 + G_i)$. Furthermore,

$$P_{ij}^s = \Pr\{\text{transmission } \langle i, j \rangle \text{ is successful}\}$$

$= \Pr\{j \text{ and its neighbors excluding } i \text{ are idle at start of reception and no node in}$

$N(j)$ transmits during the transmission $\langle i, j \rangle\}$.

Let $N'(j) = N(j) - i$. Then

$$P_{ij}^s = \prod_{l \in N'(j)} \left(\frac{1}{1 + G_l} \right) \prod_{k \in N'(j)} e^{-G_k},$$

$$c_{ij} = G_{ij} \prod_{l \in N(j)} \left(\frac{1}{1 + G_l} \right) \prod_{k \in N'(j)} e^{-G_k},$$

$$\begin{aligned}
c_i &= \sum_{j \in N^*(i)} G_{ij} \prod_{l \in N(j)} \left(\frac{1}{1 + G_l} \right) \prod_{k \in N'(j)} e^{-G_k}, \\
&= \sum_{j \in N^*(i)} G_{ij} \prod_{l \in N(j)} \left(\frac{1}{1 + G_l} \right) \exp\left(- \sum_{k \in N'(j)} G_k\right),
\end{aligned}$$

For the case of the regular topologies (with degree d), $G_i = G$ and $c_i = c(G) \forall i$. Hence the nodal capacity is expressed as

$$c(G) = \frac{G}{(1 + G)^{d+1}} e^{-dG},$$

is maximized by

$$G = \sqrt{\frac{d+1}{d}} - 1$$

and hence the optimum nodal capacity is expressed as

$$c(G^*) = \left(\sqrt{\frac{d}{d+1}} \right)^{d+1} \frac{\sqrt{d+1} - \sqrt{d}}{\sqrt{d}} e^{-(\sqrt{d^2+d} - d)}, \quad (6)$$

Slotted ALOHA: Note that $P_i^I = 1, \forall i$.

$$\begin{aligned}
P_{ij}^s &= \prod_{k \in N'(j)} (1 - G_k) \\
S_{ij} &= \frac{1}{1 + a} G_{ij} \prod_{k \in N'(j)} (1 - G_k).
\end{aligned}$$

For the case of regular topologies (with degree d), the nodal capacity is expressed as

$$c(G) = \frac{1}{1 + a} G(1 - G)^d.$$

This is maximized by $G = 1/(1 + d)$, and hence

$$\begin{aligned} c(G^*) &= \frac{1}{1+a} \frac{1}{d+1} \left(1 - \frac{1}{d+1}\right)^d \\ &= \frac{1}{(1+a)(d+1)} \left(\frac{d}{d+1}\right)^d. \end{aligned}$$

Appendix 2: Capacity Analysis of CSMA, C-BTMA and CASMA in Fully Connected Topologies

CSMA: Using renewal theory arguments as in [3], the nodal capacity is expressed as

$$c_{CSMA}(G) = \frac{1}{N} \frac{E(U)}{E(B) + E(I)}$$

where $E(\cdot)$ denotes the expected value, U denotes the channel utilization, B denotes the busy period, and I denotes the idle period. It is assumed that N is large in calculating the expected busy period.

In CSMA (for $N > 1$), the above quantities are expressed as

$$E(U) = e^{-a(N-1)G},$$

$$E(I) = \frac{1}{NG},$$

$$E(B) = 1 + 2a - \frac{1}{(N-1)G} (1 - e^{-a(N-1)G})$$

Hence,

$$\begin{aligned} c_{CSMA}(G) &= \frac{1}{N} \frac{e^{-a(N-1)G}}{\frac{1}{NG} + 1 + 2a - \frac{1}{(N-1)G} (1 - e^{-a(N-1)G})} \\ &= \frac{1}{N} \frac{(N-1)G e^{-a(N-1)G}}{\frac{N-1}{N} + (1+2a)(N-1)G - (1 - e^{-a(N-1)G})}. \end{aligned}$$

Note that for N large, the network capacity is expressed as

$$C_{CSMA}(g) = \frac{g e^{-ag}}{(1+2a)g + e^{-ag}},$$

where we have set $g = (N-1)G$. This is the same expression as in [3], where it was assumed that the generation process of the entire population of nodes constituted a Poisson process of rate g .

C-BTMA: The analysis for this case is very similar to that for the case of CSMA. For $N > 2$, the only difference is the fact that the period of time for which nodes are blocked is longer by an additional amount a , due to the busy-tone. Hence

$$c_{C-BTMA}(G) = \frac{1}{N} \frac{(N-1)G e^{-a(N-1)G}}{\frac{N-1}{N} + (1+3a)(N-1)G - (1 - e^{-a(N-1)G})}.$$

CASMA: In this case, both the vulnerable period and the period of time for which nodes are blocked are longer by an additional amount a as compared to C-BTMA. In this instance for $N > 2$

$$E(U) = e^{-aG(2N-3)},$$

$$E(I) = \frac{1}{NG},$$

$$E(B) = 1 + 4a - \frac{e^{-aG(N-2)}}{(N-1)G} (1 - e^{-aG(N-1)}) - \frac{1}{(N-2)G} (1 - e^{-aG(N-2)})$$

Hence

$$c_{CASMA}(G) = \frac{(N-1)(N-2)G e^{-aG(2N-3)}}{(N-1)[N(N-2)(1+4a)G - 2] + N e^{-aG(N-2)} + N(N-2)e^{-aG(2N-3)}}.$$

References

- [1] F. Tobagi, "Multiaccess Protocols in Packet Communication Systems," *IEEE Trans. Commun.*, Vol. COM-28, No. 4, April 1980, pp468-488.
- [2] N. Abramson, "The ALOHA system - Another Alternative for Computer Communication," *1970 Fall Joint Comput. Conf. AFIPS Conf. Proc.*, Vol. 37, pp281-285.
- [3] L. Kleinrock and F. Tobagi, "Packet Switching in Radio Channels: Part 1 - Carrier Sense Multiple-Access Modes and their Throughput-Delay Characteristics," *IEEE Trans. Commun.*, Vol. COM-23, No. 12, December 1975, pp1400-1416.
- [4] F. Tobagi and L. Kleinrock, "Packet Switching in Radio Channels: Part 2 - The Hidden Terminal Problem in Carrier Sense Multiple-Access and the Busy-Tone Solution," *IEEE Trans. Commun.*, Vol. COM-23, No. 12, December 1975, pp1417-1433.
- [5] P. Spilling and F. Tobagi, "Activity Signalling and Improved Hop Acknowledgements in Packet Radio Systems," *PTRN 283*, January 1980.
- [6] R. Kahn, S. Gronemeyer, J. Burchfiel and R. Kunzelman, "Advances in Packet Radio Technology," *Proc. IEEE*, Vol. 66, Nov. 1978, pp1468-1496.
- [7] F. Tobagi, "Analysis of a Two-Hop Centralized Packet Radio Network—Part I: Slotted ALOHA," *IEEE Trans. Commun.*, Vol. COM-28, No. 2, February 1980, pp196-207.
- [8] F. Tobagi, "Analysis of a Two-Hop Centralized Packet Radio Network—Part II: Carrier Sense Multiple Access," *IEEE Trans. Commun.*, Vol. COM-28, No. 2, February 1980, pp208-216.

- [9] R. Boorstyn and A. Kershenbaum, "Throughput Analysis of Multihop Packet Radio," *Proceedings of ICC*, Seattle, June 1980, pp 13.6.1- 13.6.6.
- [10] F. Tobagi and J. Brazio, "Throughput Analysis of Multihop Packet Radio Networks Under Various Channel Access Schemes," *Proc. INFOCOM*, San Diego, May 1983.
- [11] R. Boorstyn , A. Kershenbaum and V. Sahin, "A new Acknowledgement Protocol for Analysis of Multihop Packet Radio Networks," *Proceedings of COMPCON*, Washington, 1982.
- [12] J. Brazio and F. Tobagi, "Theoretical Results in Throughput Analysis of Multihop Packet Radio Networks," *Proc. ICC*, Amsterdam, May 1984.
- [13] J. Brazio and F. Tobagi, "Throughput Analysis of Spread Spectrum Multihop Packet Radio Networks," *Proc. INFOCOM*, Washington, DC., March 1985.
- [14] B. Maglaris, R. Boorstyn and A. Kershenbaum, "Extensions to the Analysis of Multihop Packet Radio Networks," *Proc. INFOCOM*, San Diego, California, May 1983.
- [15] H. Takagi, "Analysis of Throughput and Delay for Single- and Multi-hop Packet Radio Networks," *UCLA report No. CSD-830523*, May, 1983.
- [16] F. Tobagi and J. Storey, "Improvements in Throughput of a CDMA Packet Radio Network due to a Channel Load Sense Access Protocol," *22nd Allerton Conf.*, Urbana, ILL, October, 1984.
- [17] M. Gerla and L. Kleinrock, "Flow Control: A Comparative Survey," *IEEE Trans. Commun.*, Vol. COM-28, No. 4, April 1980, pp553-574.

- [18] F. Tobagi, R. Binder and B. Leiner, "Packet Radio and Satellite Networks," *IEEE Communications Magazine*, Vol. 22, No. 11, pp24-40, November 1984.
- [19] J. Silvester and L. Kleinrock, "On the Capacity of Multihop Slotted ALOHA Networks with Regular Structure," *IEEE Trans. Commun.* Vol. COM-31, No. 8, August 1983, pp974-982.
- [20] L. Kleinrock and S. Lam, "Packet switching in a multiaccess broadcast channel: Performance evaluation," *IEEE Trans. Commun.*, Vol. COM-23, pp410-423, Apr. 1975.